



Research Progress of Fabrics with Different Geometric Structures for Triboelectric Nanogenerators in Flexible and Wearable Electronics

Dali Yan¹ · Jian Ye¹ · Yahui Zhou¹ · Xingxin Lei¹ · Bo Deng¹ · Weilin Xu¹

Received: 31 May 2023 / Accepted: 12 September 2023 / Published online: 16 October 2023
© Donghua University, Shanghai, China 2023

Abstract

Widespread reliance on fossil fuels, and the resulting imbalance between energy supply and demand have emerged as significant obstacles to achieving sustainable development. Triboelectric nanogenerators (TENGs) offer a viable solution to this problem. Among the various materials used in TENGs, fabrics with geometric structures have attracted considerable interest because of their advantageous properties, such as their light weight, breathable structures, favorable softness, and excellent breathability. This review provides a comprehensive introduction to fabric geometric (fabric structure with yarn as the basic unit, including woven fabrics formed by warp and weft yarns and knitted fabrics formed by yarn coils, etc.) TENGs, including their definition, working principle, and mechanisms, and explores the recent progress in TENGs based on one-, two-, and three-dimensional structures, classifying them into woven and knitted fabrics according to the fabrication method. We summarize the advantages and disadvantages of TENGs with different dimensions. Considering the intrinsically limited conductivity of the fiber and fabric, progress in improving the comprehensive output performance of TENGs via combination with other conductive materials and surface modification is discussed. Finally, this review concludes with a discussion of the challenges, opportunities, and potential applications related to TENGs based on fabric geometric structures. This study is expected to provide readers with new strategies and conceptual ideas to improve the performance of TENGs constructed with fabrics, particularly through the optimization of their structures.

Keywords Geometric structure · Triboelectric nanogenerators · Dimensional · Fabric-based

Introduction

The excessive use of fossil fuels and growing energy demand in various fields have impeded the sustainable development of human societies [1, 2]. Various new renewable energy sources, including wind [3–6], water flow [7–10], collision [11], and human motion energy [12–14], have emerged as feasible solutions for alleviating this problem. Triboelectric nanogenerators (TENGs)—based on electrostatic induction and frictional initiation coupling—can efficiently harvest

various types of mechanical energy wasted in nature and life [15]. In addition, TENGs combined with wearable devices overcome the disadvantages of traditional rigid batteries, including their large size, short lifespan, and frequent recharging. TENGs have advantages over rigid batteries in both supplying energy for wearable devices and harvesting bioenergy [16–20].

TENGs can be categorized into four basic modes of operation: vertical contact–separation [21–23], lateral sliding [24–26], single electrode [27–30], and freestanding triboelectric layer [31]. The vertical contact–separation mode, which is the dominant motion of human activities and can be easily realized through the fabric's rich structures, is considered the most suitable carrier for collecting mechanical energy from daily human movement [32]. Therefore, one of the main goals in the development of wearable electronic devices is to integrate them with fabrics, ensuring device functionality while maintaining fabric softness, comfort, and breathability [33]. In recent years, numerous studies have focused on TENGs with fabric geometric structures,

Dali Yan and Jian Ye have contributed equally to this article.

✉ Bo Deng
dengjianguo88@outlook.com

Weilin Xu
weilin_xu@hotmail.com

¹ State Key Laboratory of New Textile Materials and Advanced Processing Technologies, Wuhan Textile University, Wuhan 430200, China

revealing the intricate relationships between the material properties and geometric structures of TENGs and their output performance [34, 35].

As shown in Fig. 1, fabric geometric TENGs have undergone significant and rapid development in recent years, with numerous articles describing their structure and material design [36]. Different materials have different properties, leading to the selection of various dielectric materials as friction materials. For the electrodes, low-resistance metals or coated materials containing carbon are typically used as dielectrics to guide the induced charge. It is essential to maintain fabric comfort and breathability when introducing electrode materials to fabric geometric TENGs. In this review, we classify them according to their dimensions and

fabrication methods. The properties of the different composite materials and surface modifications are discussed. Finally, current challenges with fabric geometric TENGs are addressed, and future research directions in textile technology are proposed. This review aims to provide valuable insights for researchers studying fabric geometric TENGs.

Fundamental Theory of TENGs

Definition and Working Principle of TENGs

When two different frictional materials are separated by contact under external forces, charges of opposite polarity are generated on their surfaces because of electrostatic induction and frictional initiation, resulting in a potential difference. The electrons flow back and forth between the two electrodes in the external circuit through the load to balance the potentials, forming a current. This process converts mechanical energy into electrical energy [55].

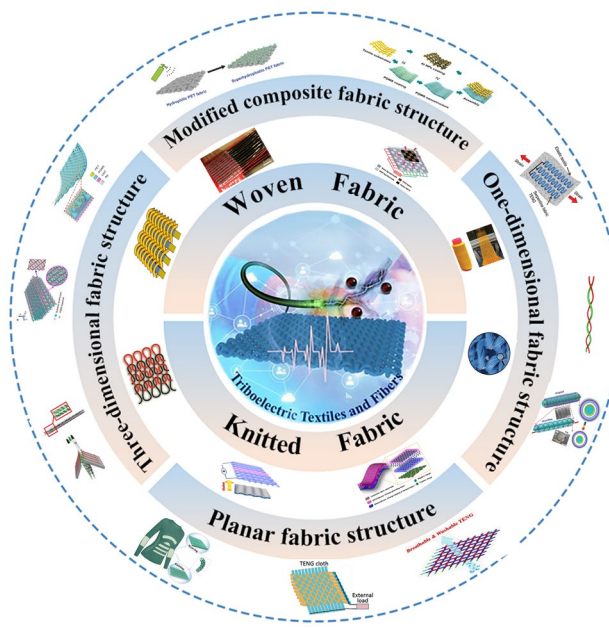


Fig. 1 Classification of fabric geometric TENGs; Reproduced with permission from ref [33], Copyright 2016, WILEY–VCH. Reproduced with permission from ref [37], Copyright 2014, American Chemical Society. Reproduced with permission from ref [38], Copyright 2017, American Chemical Society. Reproduced with permission from ref [39], Copyright 2015, WILEY–VCH. Reproduced with permission from ref [40], Copyright 2018, Royal Society of Chemistry. Reproduced with permission from ref [41], Copyright 2022, John Wiley & Sons. Reproduced with permission from ref [42], Copyright 2019, Elsevier. Reproduced with permission from ref [43], Copyright 2019, Elsevier. Reproduced with permission from ref [44], Copyright 2020, Springer Nature. Reproduced with permission from ref [45], Copyright 2018, Elsevier. Reproduced with permission from ref [46], Copyright 2016, Springer Nature Limited. Reproduced with permission from ref [47], Copyright 2021, WILEY–VCH. Reproduced with permission from ref [48], Copyright 2022, Elsevier. Reproduced with permission from ref [49], Copyright 2015, Elsevier. Reproduced with permission from ref [9], Copyright 2017, WILEY–VCH. Reproduced with permission from ref [50], Copyright 2021, Elsevier. Reproduced with permission from ref [51], Copyright 2020, WILEY–VCH. Reproduced with permission from ref [52], Copyright 2022, Elsevier. Reproduced with permission from ref [53], Copyright 2019, Elsevier. Reproduced with permission from ref [54], Copyright 2023, WILEY–VCH

Operating Modes of TENGs

TENGs have four operation modes (Fig. 2): vertical contact–separation [56–58], lateral sliding [19, 30, 31], single-electrode [40, 41, 43], and freestanding triboelectric layer [42, 59, 60]. The applications of these four basic operating modes, either individually or in combination, result in a wide variety of TENGs. Weaving and knitting are convenient for preparing single- or multi-layer fabrics, making it easy to fabricate TENGs that combine different operation modes.

Vertical Contact–Separation Mode

Vertical contact–separation TENGs have a basic ‘sandwich’ structure that relies on the effective separation of two friction layers in the vertical direction. The change in the spacing between the friction layers generates inductive charges. The three-dimensional (3D) structure of the spacer or multi-layer fabric combines the resilience and flexibility of the fabric, so that the spacer layer remains stable after high-frequency deformation in the vertical direction. It demonstrates the great potential of 3D-structured fabrics in harvesting human energy dominated by vertical motion and supplying power to wearable devices [61, 62].

Lateral-Sliding Mode

Lateral-sliding TENGs consist of two friction layers that slide relative to each other, generating charge due to the changing distance between their centers. Electrons flow

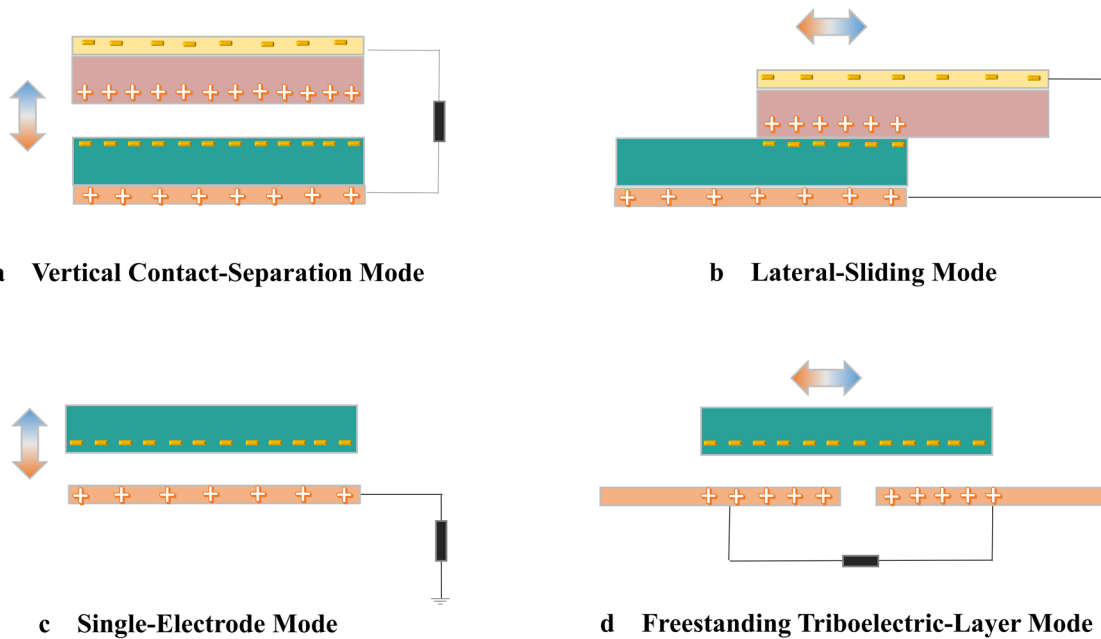


Fig. 2 Four operation modes of TENGs

through the outer circuit to counteract the potential difference. As they do not need a vertical airgap, these TENGs can be easily integrated onto clothing surfaces and harvest the mechanical energy generated by human motion [56, 57], giving them a wide range of applications in sensing [25, 26].

Single-Electrode Mode

Single-electrode TENGs consist of a directly grounded single electrode. Electrons move on the circuit formed by the Earth and the bottom electrode to generate current. When embedded in clothing, the TENG efficiently converts mechanical energy into electrical energy through friction with the skin [58, 61, 63]. This technology can also be used in electronic skin applications [62, 64].

Freestanding Triboelectric-Layer Mode

The freestanding triboelectric-layer TENG involves an object that slides reciprocally in the friction layer, causing an uneven charge distribution on the symmetric electrodes at the back of the two friction layers. Then, electrons generate a current by balancing the potentials at the two ends of the load. Compared with the lateral-sliding TENG, this TENG reduces friction, prolongs the service life, and provides a novel solution for powering wearable devices [37, 41].

Working Mechanism of TENGs

The mechanisms of induction and friction between two dielectric surfaces are complex. When considering the mechanism of TENGs, we must consider the types of charge transfer between different dielectrics and the forces that drive the charge transfer. Using advanced detection techniques, charge-transfer mechanisms can be broadly categorized into three types: electron transfer, ion transfer, and material particle transfer. The corresponding mechanisms are explained below.

Electron Transfer

Wang et al. [65] proposed an electron cloud overlap model (Fig. 3) in which two atoms forming a bond have an equilibrium distance representing their bond length or interatomic distance. Initially, the electron clouds between them remain separated with no overlap (Fig. 3a). However, when an external force is applied, the two atoms come into contact, resulting in an interatomic distance x less than their bond length and an overlap of the electron clouds or wave functions (Fig. 3b). This overlapping electron cloud lowers the energy barrier between the two atoms, facilitating electron transfer from one atom to another. After separation, the transferred electrons remain as electrostatic charges on the material surface (Fig. 3c).

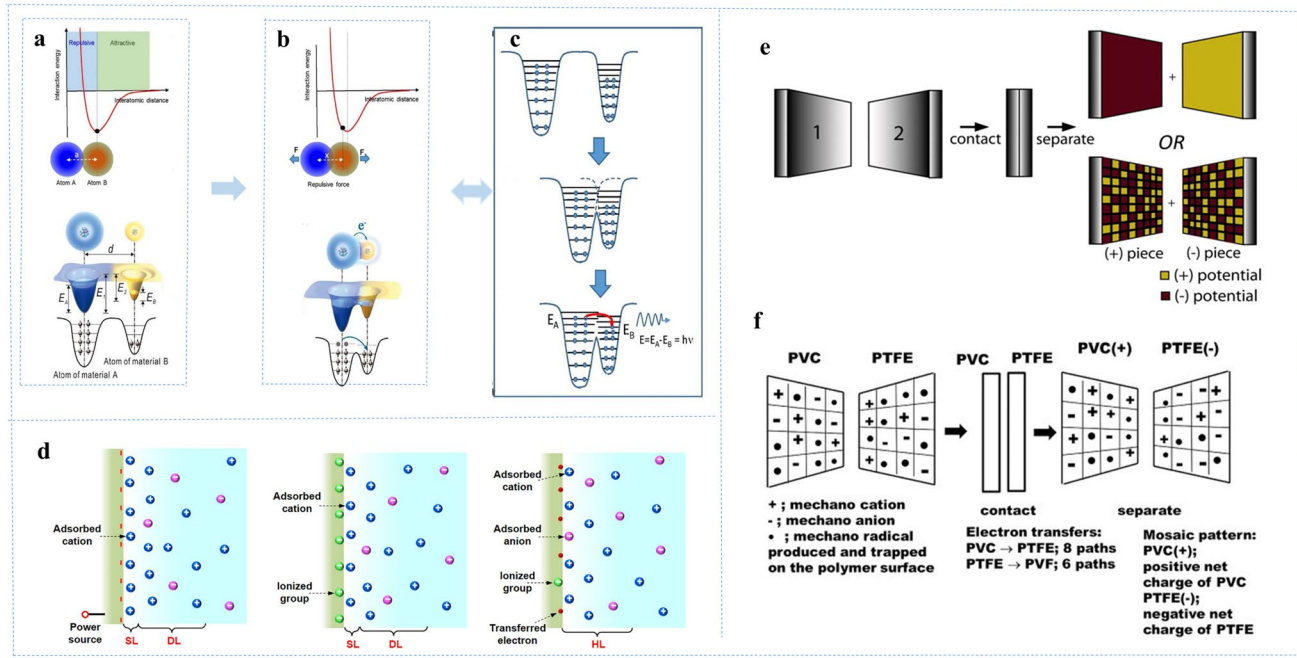


Fig. 3 TENG mechanism with electron cloud overlap modeling of two atoms: analytical electron cloud potential energy profiles: **a** before, **b** during, and **c** after contact; reproduced with permission from ref [65], Copyright 2019, Elsevier. **d** Charge distribution on the surface of the ion-transferring liquid–solid surface; reproduced with permission from ref [70], Copyright 2020, American Chemical Society

Ion Transfer

Ion transfer refers to the migration of ions from one material to another. This process involves the asymmetric separation of ions, which leads to the generation of frictional charges. For example, Wang et al. proposed an electrical double-layer model to explain solid–liquid interfaces. In this model, an object is surrounded by two layers of parallel charges. The first layer—called the surface charge—is created when liquid molecules impact the solid surface owing to thermal motion or liquid pressure. A cloud of overlapping electrons is generated by the interaction between the liquid molecules and the molecules on the solid surface. The second layer consists of ions attracted to the surface charge via Coulomb forces while being shielded from the first layer. These ions are free and driven by thermal motion to move through the fluid rather than being tightly bound together (Fig. 3d) [66].

Material Particle Transfer

Material particle transfer is not the primary mechanism of frictional initiation, unlike electron or ion transfer. However, it explains issues that electron and ion transfer cannot address, such as contact initiation between materials of the same species [67]. According to Baytekin's proposal

entity. **e** Mosaic region of the contact charge; reproduced with permission from ref [68], Copyright 2011, The American Association for the Advancement of Science. **f** Modeling of the transfer of material particles; reproduced with permission from ref [69], Copyright 2020, American Chemical Society

depicted in Fig. 3e, when two polymer surfaces come into contact, they form a random mosaic of nanosized regions with opposite charges. Changes in this random ‘mosaic’ lead to changes in the material’s surface composition, resulting in material particle transfer between the contacting surfaces [68]. Kelvin probe force microscopy—employed to measure the patterns generated by material particle transfer—revealed that charge transfer occurred uniformly across the entire contact surface (Fig. 3f). Contact charging between the two polymers involves mass transfer as well as the breaking of covalent bonds in the polymer backbone, generating mechanical radicals, which become trapped on the material surface [69].

Classification of TENGs Based on Fabric Geometry

Fabric geometric TENGs can be classified as one-dimensional (1D), two-dimensional (2D), or 3D. Additionally, they can be categorized into woven and knitted fabrics according to the fabrication methods employed. Woven fabrics can be further divided into plain, twill, and satin fabrics, according to their basic interweaving methods. Moreover, TENGs can be classified into spacer layer structures [55],

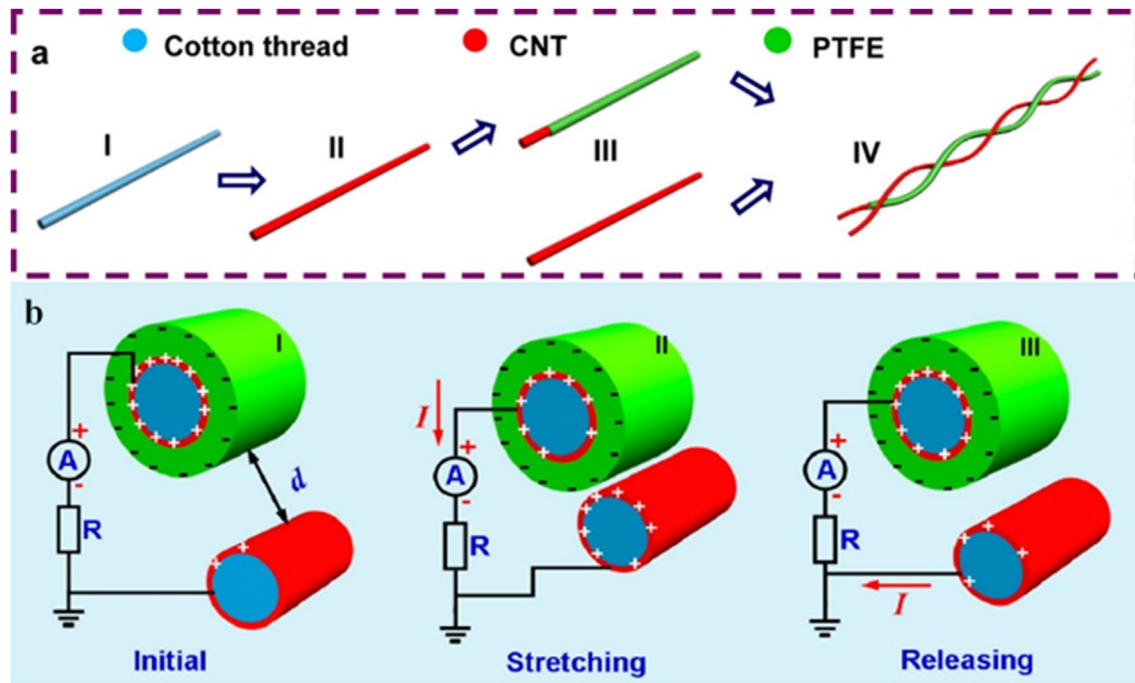


Fig. 4 **a** Fabrication method for 1D yarn TENGs with a coated structure and **b** the generator system; reproduced with permission from ref [37]. Copyright 2014, American Chemical Society

[71], ‘core–shell’ structures [61, 72], etc. according to their fabric structures.

Classification by Dimensions

TENGs Based on 1D Structures

TENGs consist of a friction and an electrode layer. The electrodes are usually made of low-resistance metals, carbon-containing coatings, or polymers. In fabric geometric TENGs, fabrics are used as both friction materials and substrates. The electrodes need to transfer charge from the friction material’s surface and must possess specific characteristics, such as softness, breathability, and compatibility with the fabric. Zhong et al. were the first to report the development of a metal-free fiber-based TENG [37]. The fabrication process, which is illustrated in Fig. 4a, involves impregnation and drying. It utilizes a cotton thread (CCT) coated with carbon nanotubes (CNTs) and a cotton thread (PCCT) coated with a combination of polytetrafluoroethylene (PTFE) and CNTs. The two modified cotton threads are intertwined to form a double-helical structure. Importantly, the CNT coating seamlessly integrates into the fabric during the weaving process, acting as an electrode layer for charge accumulation and allowing the collection of energy from finger bending and wireless temperature sensing. Each intertwined cotton thread has an electrode layer. When the CCT is grounded, the outer layer of the PCCT with the PTFE surface acquires

a negative charge Q . Through electrostatic induction, the CNTs of the PCCT and CCT carry opposite charges Q_1 and Q_2 , respectively, with $Q=Q_1+Q_2$, satisfying charge conservation. Consequently, when the gap between the PCCT and CCT changes, electrons flow back and forth through the external circuit R to balance the potentials, as shown in Fig. 4b.

In addition to yarn surface conductive modification, another approach involves fabricating conductive and friction material yarns into a core–shell structure [33]. This technique is illustrated in Fig. 5a, where silicone-coated stainless-steel conductive yarns are arranged in a serpentine pattern on an elastic textile capable of withstanding up to 100% elastic strain. Electron transfer occurs between two friction layers via contact between the silicone and skin, resulting in alternating-current (AC) open-circuit voltage generation and accumulation of transferred charge, reaching values of up to 15 V and 12 nC, respectively (Fig. 5b). This 1D-structure-based TENG, which utilizes conductive yarn as the core thread (electrode layer) and a friction material yarn as the shell thread (friction layer), has been successfully used for energy harvesting from human motion and biomedical sensing applications.

Most 1D-structure-based TENGs use fabrics as carriers (Fig. 5a). However, these 1D-yarn-based TENGs have limitations such as a single mode of energy conversion and limited sensing capabilities, which substantially hinder their application. Innovative approaches have been developed to

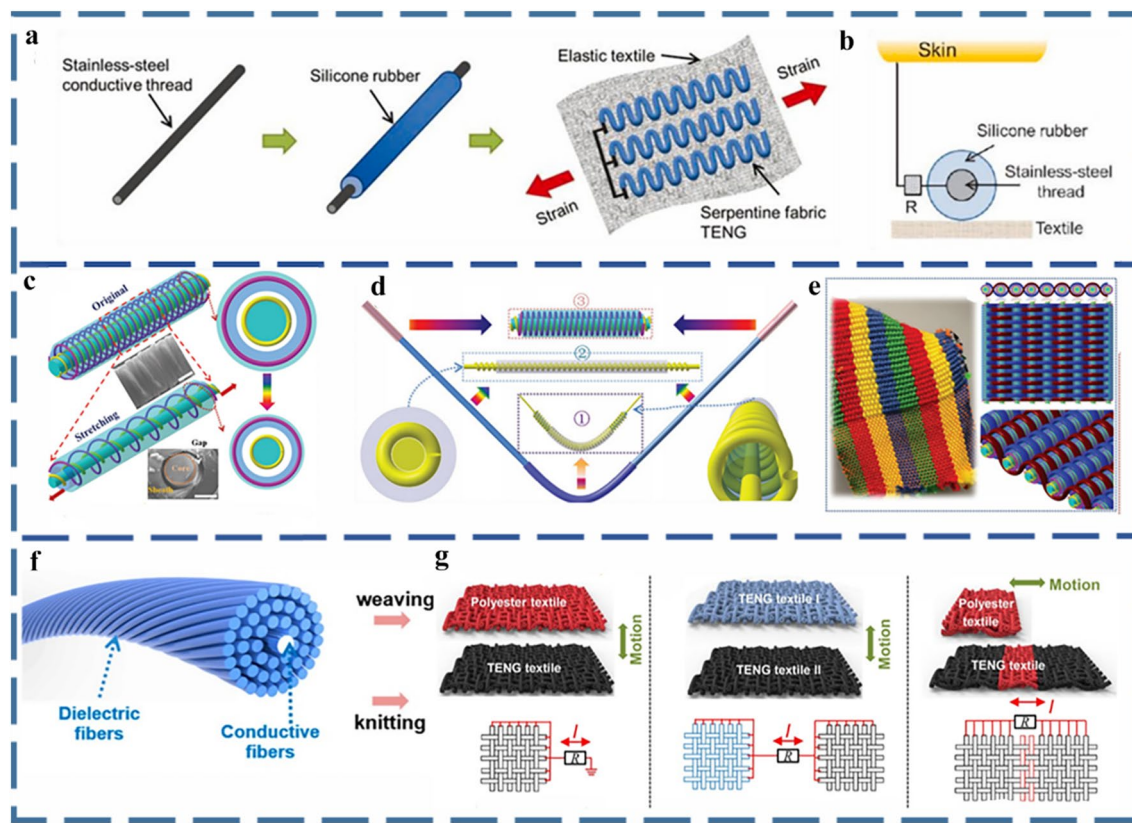


Fig. 5 Core–shell structure-based TENGs. **a** Fabrication of stretchable single-dimensional TENGs and **b** working mechanism; reproduced with permission from ref [33], Copyright 2016, WILEY–VCH. **c** Silicone-coated stainless-steel threaded yarn, **d** schematic of self-counting jump rope, and **e** large-area fabric; reproduced with permis-

sion from ref [73], Copyright 2018, WILEY–VCH. **f** Dielectric spandex fibers are covered with stainless-steel fibers and their **g** textiles; reproduced with permission from ref [38], Copyright 2017, American Chemical Society

overcome these limitations. As shown in Fig. 5c and d, modified yarns, besides serving as automatic jump rope counters, can also be woven into textiles for efficiently harvesting energy from human motion (Fig. 5e) [73]. For instance, Yu et al. [38] employed core–shell structures to create fabrics with distinctive properties (Fig. 5f). These fabrics consisted of conductive fibers covered with either manmade polymer fibers or natural fibers, allowing various modes of electrical output, e.g., single-electrode, contact–separation, and freestanding triboelectric-layer (Fig. 5g). Such advancements facilitate enhanced energy-harvesting capabilities and expand the range of applications of TENGs.

TENGs Based on 2D Structures

2D-structure-based TENGs have garnered considerable attention for their potential use in energy harvesting and self-driven sensor applications, which has been supported by influential studies. To inspire further advancements in 2D-structure-based TENGs, we present notable examples of the development and optimization of TENG electrodes

using textiles. These examples illustrate the challenges and prospects in this area.

In the previous studies, TENGs were developed using polymer films as the friction-layer materials [74, 75]. However, these materials had limitations with regard to washability, breathability, and compatibility with clothing [76, 77]. When transitioning from 1D structures to 2D structures, although marginal performance improvements have been achieved [39], 2D TENGs face challenges related to the limited contact area and low frictional charge [78]. To address these issues, researchers have explored alternative approaches, replacing films with narrow polymer or cloth strips as friction materials using various methods.

As shown in Fig. 6a, friction materials such as nylon or polyester fabric are affixed to both sides of the conductive silver fiber strip, resulting in an area of fabric through the interweaving of the warp and weft. The friction material in the warp direction is connected to one pole using conductive fibers, and the friction material in the weft direction is connected to the other pole using conductive fibers. Electrons flow between the two poles through the load [59].

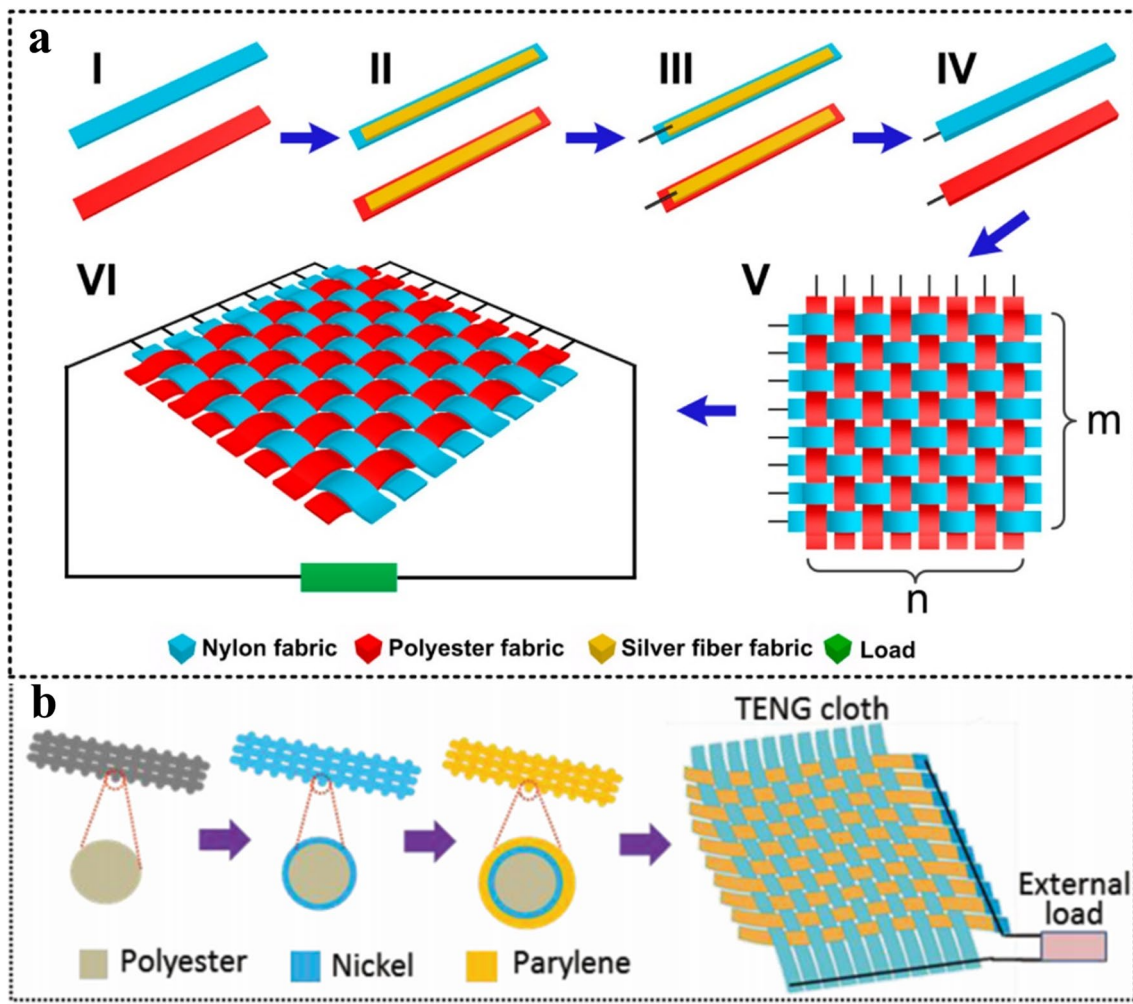


Fig. 6 2D-structure-based TENGs based on the strip woven structure: **a** electrode and friction material paste-type strip woven structure; reproduced with permission from ref. [59], Copyright 2014, Ameri-

can Chemical Society. **b** Electrode surface coated with the friction material-type strip woven structure; reproduced with permission from ref. [39], Copyright 2015, WILEY-VCH

Additionally, 2D area fabrics can be created by applying a coating of conductive material to the surface of friction material fibers (Fig. 6b) [75]. The construction of warp–weft interwoven 2D-structure-based TENGs using strips made of different materials introduces various possibilities, such as harvesting mechanical energy from the human body and wind energy from nature [60, 78].

Although the fabrication of 2D-structure-based TENGs using the strip-interweaving structure is relatively straightforward, it presents challenges. First, the friction between strips can cause deformation, leading to unstable electrical properties. Moreover, the conductive media coated on the strip surfaces are prone to peeling off because of the friction [76]. Furthermore, strip weaving is limited to hand weaving and cannot be applied to other textile-forming methods, making large-scale production unfeasible. To address these issues, researchers have modified single yarns and directly

woven them into TENGs with various weaving patterns. Figure 7a illustrates a design in which a copper strip wrapped with PTFE was woven into a plain fabric using a loom and then sewn onto the waist of a cotton lab coat, as shown in Fig. 7b. This plain fabric, which operated in the single-electrode mode at a 30 Hz impact frequency, achieved an average peak voltage of 780 V and a current of 4.9 μ A, as shown in Fig. 7c. The design also exhibited remarkable stability, overcoming the disadvantages associated with the peeling of the coating when the fabric surface is rubbed [40].

The TENG electrodes play a crucial role in exporting charge from the friction layer, which is particularly important for fabric geometric TENGs, because the electrodes need to ensure the stable exporting of friction-layer charges as well as the maintenance of the fabric's softness, comfort, and breathability. Traditional core electrodes made of metals such as aluminum and copper are less flexible and are

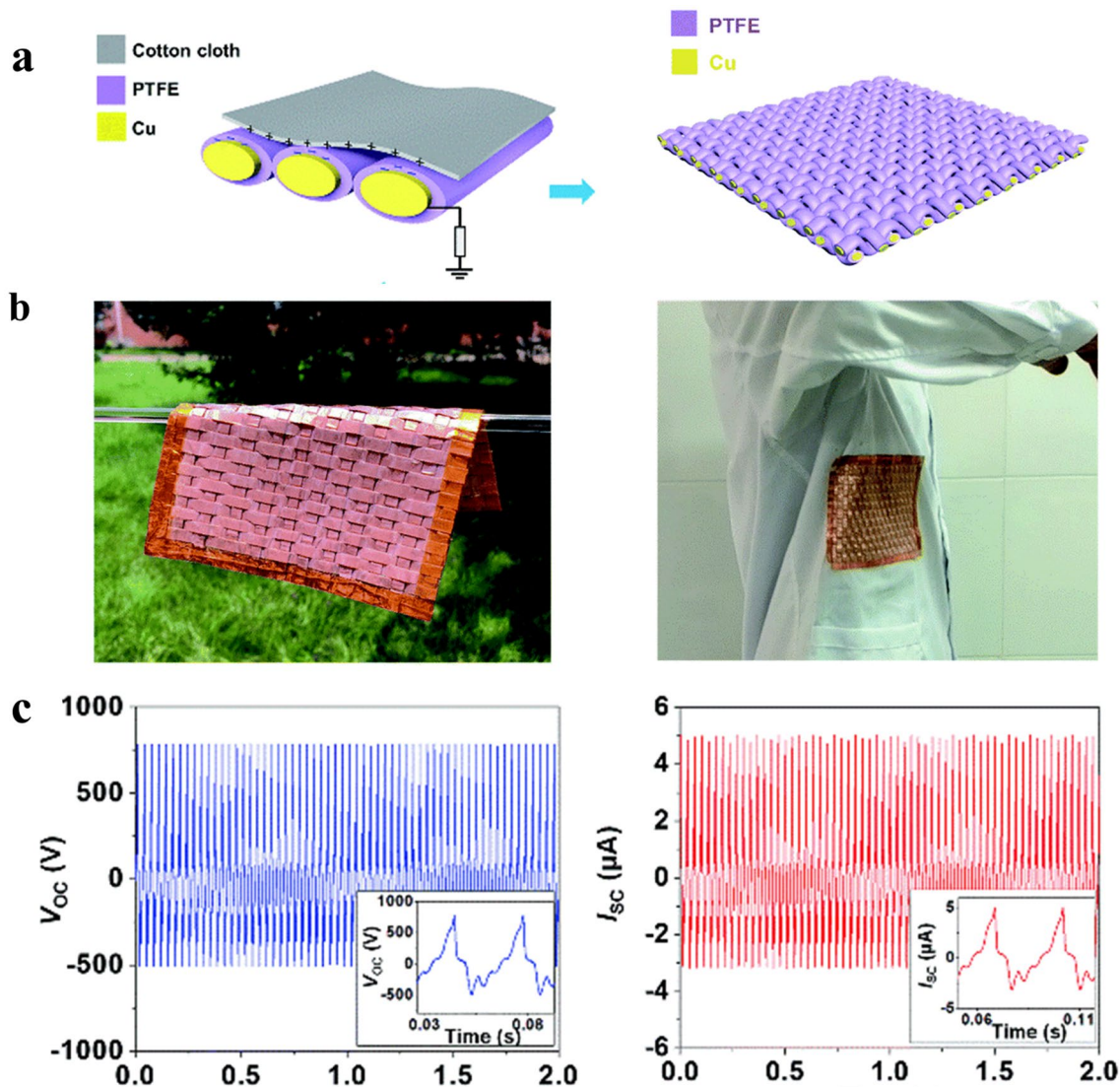


Fig. 7 **a** Schematic of plain fabric with the metal electrode, **b** photograph of plain fabric with the metal electrode, and **c** output voltage and current of plain fabric (5 cm × 5 cm) at a 30 Hz frequency; reproduced with permission from ref [40], Copyright 2018, Royal Society of Chemistry

prone to fatigue and fracture as the fabric deforms [79, 80]. To address these challenges, Li et al. [41] used a high-speed braiding machine to fabricate silver-plated conductive yarns with polyvinylidene fluoride (PVDF) yarns (Fig. 8a). This process resulted in the production of core–shell-structured yarns that could be manufactured on a large scale and wound continuously on a spindle (Fig. 8b and c). Scanning electron microscopy (SEM) images of the core–shell fibers revealed that the friction material, i.e., the PVDF yarn, was neatly wrapped around the silver-plated conductive yarn without breakage (Fig. 8d and e). Additionally, Li et al. explored knitting and weaving techniques for incorporating the core–shell-structured yarn into the fabric (Fig. 8f). Figure 8g illustrates the charge transfer when the core–shell yarn comes into contact with the skin or other friction materials,

operating in the single-electrode mode. This setup yields high performance with regard to the power output (V_{OC} of 26 V, Q_{SC} of 8.5 nC, I_{SC} of 129 nA at 3 Hz). These textile-based TENGs have considerable potential for energy harvesting and pressure detection, as they significantly reduce the impact of the external environment on the coatings.

Furthermore, researchers have found that flexible electrode materials used in fabric geometric TENGs, such as those coated with silver nanowires or doped with CNTs, exhibit a higher internal resistance and lower conductivity than metals. When the internal resistance is far higher than the resistance of the external circuit, the total current and the external circuit voltage are low owing to the dominance of the internal resistance in the overall pathway resistance, which limits the practical applications of these materials. Jing

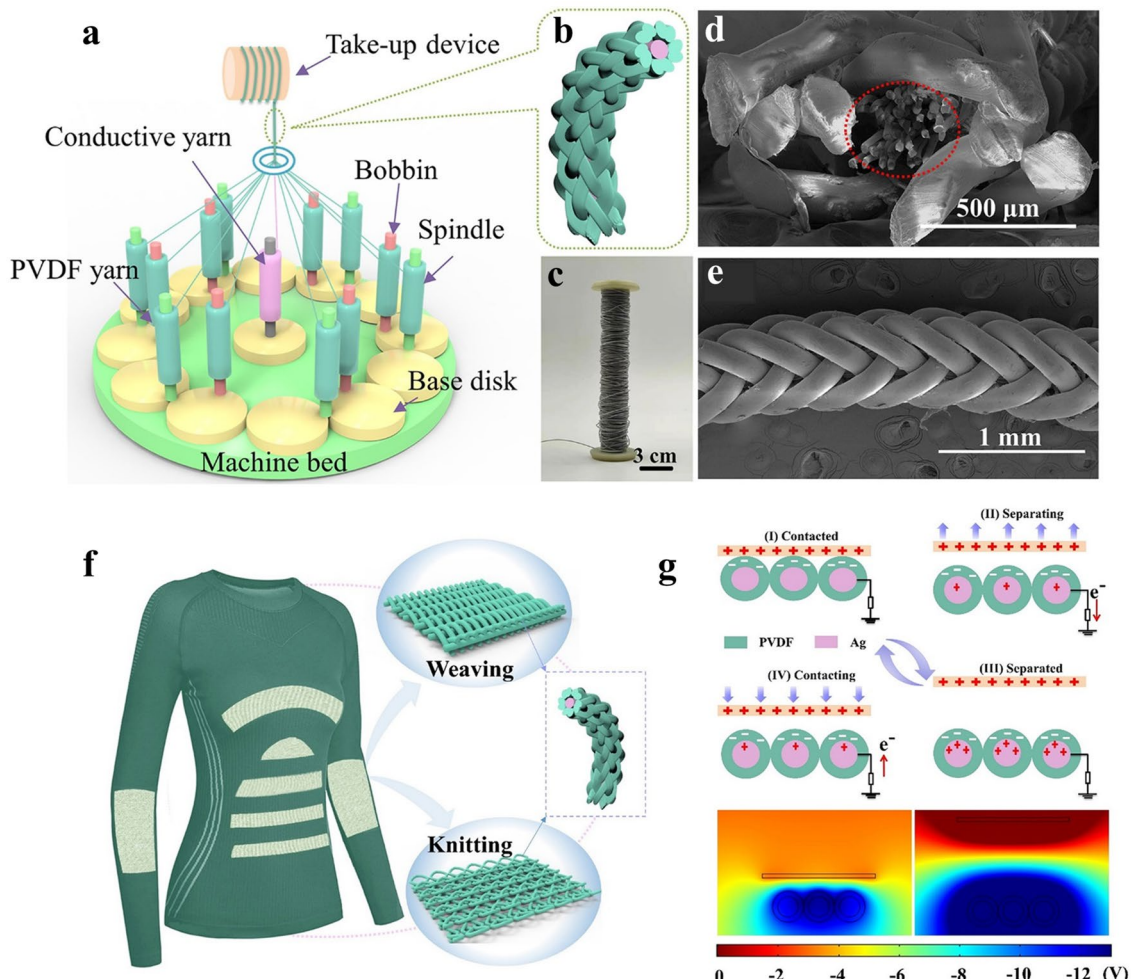


Fig. 8 Core–shell-structured yarn for energy harvesting: **a** schematic of the high-speed rope knitting machine, **b** structure of core–shell yarn, **c** photograph of core–shell yarn, **d** SEM image of the core–shell yarn cross-section, **e** SEM image of the core–shell yarn surface mor-

phology, **f** schematic of core–shell TENGs with different structures on garments, and **g** working-principle diagram and COMSOL simulation of core–shell TENGs; reproduced with permission from ref [41], Copyright 2022, John Wiley & Sons

et al. [79] addressed the high resistance of flexible electrodes by adopting a physical series–parallel structure of electrode fibers, which comprised a stretchable core and a silica gel shell (Fig. 9a). The triboelectricity and electrostatic induction occurring between the silicone rubber and external polyimide film because of their different electron gain and loss abilities are depicted in Fig. 9b. To maintain the overall electrostatic balance, electrons circulate in the circuit, generating current; this configuration leads to significant improvements—particularly for long fibers. As shown in Fig. 9c, the parallel multi-fiber structure exhibits a lower resistance and higher current than the fiber-shaped electrodes with long length or diameter. The parallel type achieves an 11.8-fold increase in the output current compared with the single-length type, owing to a ten-fold reduction in the internal resistance.

Guan et al. [42] conducted a groundbreaking study on woven-structured TENGs. They implemented a woven parallel

structure using an electrostatically spun stainless-steel yarn as the core and electrostatically spun PA66 or P(VDF-TrFE) nanofibers as the shell (Fig. 10a). To enhance the performance of the TENGs, micro- and nanostructures were incorporated on the surface of the friction material (Fig. 10b). The resulting woven-structured TENGs, which measured $5 \times 5 \text{ cm}^2$ with a load resistance of $10 \text{ M}\Omega$, exhibited remarkable electrical characteristics (Fig. 10c). They achieved an impressive open-circuit voltage of 96 V, a short-circuit current of $8.5 \mu\text{A}$, and an instantaneous power density of 93 mW/m^2 . Considering the exceptional output power of these TENGs and the inherent advantages of nanofibers and textiles, they are ideal for biomechanical energy harvesting and self-powered sensing applications (Fig. 10d).

Although fabric geometric TENGs have considerable potential for harvesting bioenergy and self-powered sensing, there is room for improvement with regard to energy storage. Pu et al.

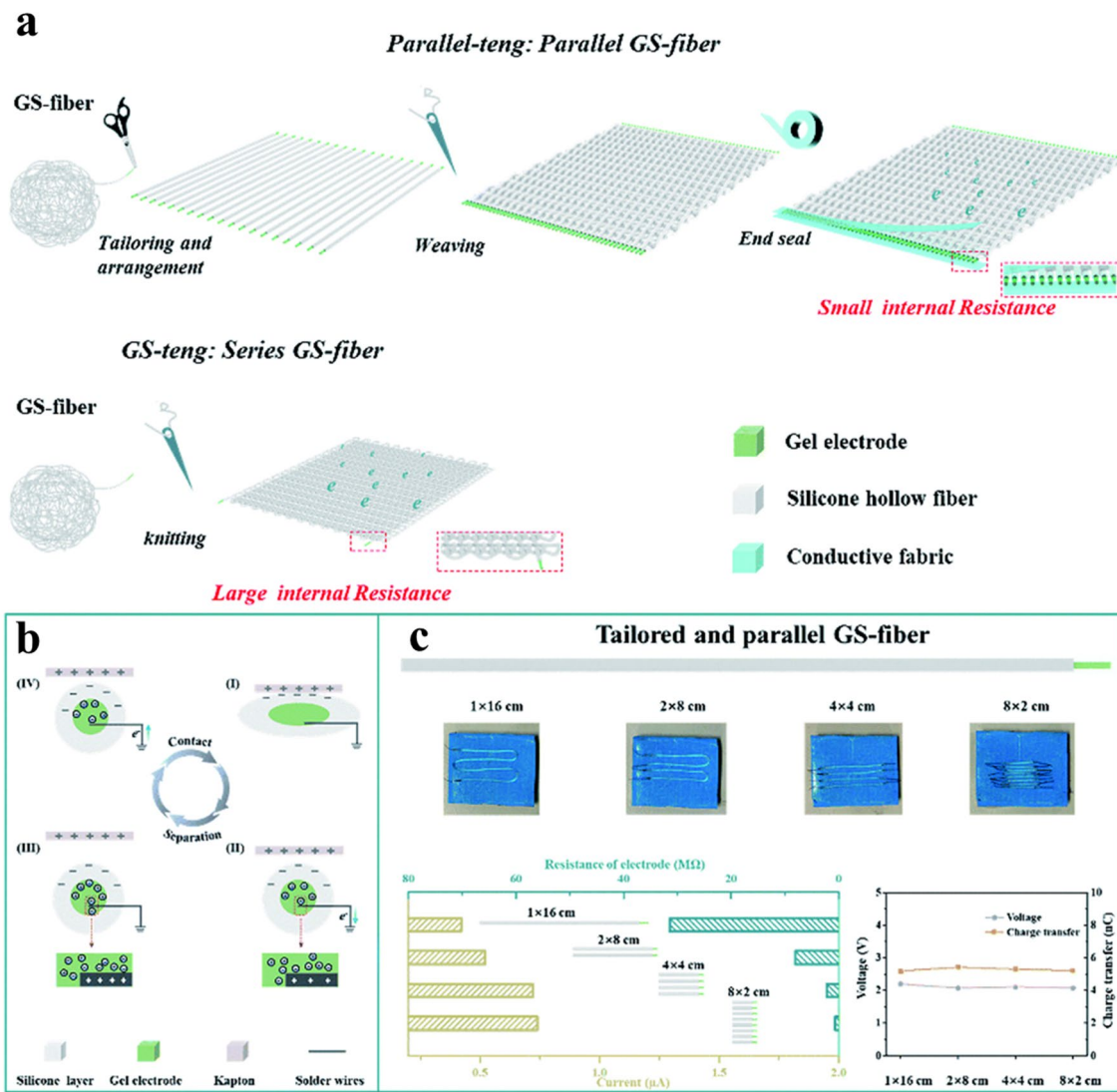


Fig. 9 Electrode fibers in the series–parallel structure: **a** multi-fiber and single-fiber structures, **b** working mechanism, **c** resistance, short-circuit current, output voltage, and short-circuit transfer charge of

electrode fibers with different parallel structures; reproduced with permission from ref [79], Copyright 2021, Royal Society of Chemistry

addressed this challenge by integrating 1D yarn capacitors and TENGs into a single fabric without compromising comfort. They achieved voltage enhancement through a series structure and increased the current via parallel connections, resulting in a remarkable energy-transfer efficiency of 72.4% between the TENGs and capacitors. Moreover, because there is a significant difference between the internal resistance of TENGs and the resistance of energy-storage devices, optimization of impedance matching and electrical design between TENGs and devices is an important direction for future development [81].

TENGs Based on 3D Structure

A 3D-structured TENG is made by incorporating a yarn system or structure in the thickness direction [82]. These fabrics

are created through weaving and knitting techniques. The simplest form of the 3D-structure-based TENG is prepared by sewing together 2D fabrics in a vertical direction. The reliability of 3D-structure-based TENGs was demonstrated by constructing devices that can power a liquid–crystal display (LCD) and 49 light-emitting diodes (LEDs) without the need for energy storage or rectification circuits [58].

Typically, 3D-structure-based TENGs consist of three layers: friction, electrode, and spacer. They primarily operate in the freestanding triboelectric-layer mode. Wearable devices based on vertical contact are promising, as vertical motion is an important component of human activity. In this mode, maintaining stable contact and separation between the different friction materials is crucial for generating consistent electrical properties. This process requires a spacer

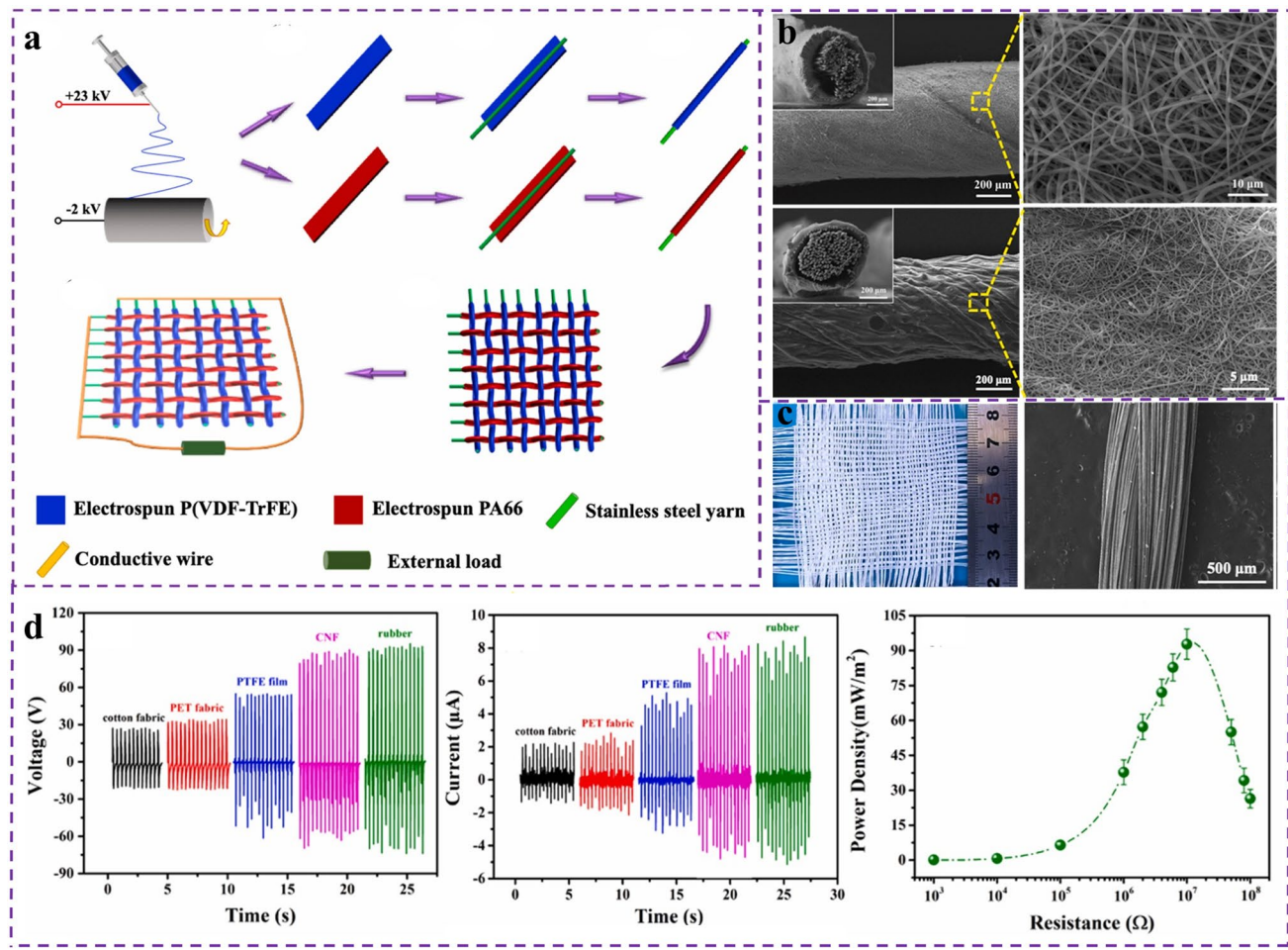


Fig. 10 Parallel structure of fabric geometric TENGs: **a** fabrication process, **b** low- and high- magnification SEM images of cross sections and surfaces of electrostatically spun P(VDF-TrFE)-SSL, **c** photogram and SEM image of stainless-steel yarn, and **d** open-circuit

voltage, short-circuit current, and power density versus load resistance curves for different materials; reproduced with permission from ref [42], Copyright 2019, Elsevier

layer with suitable elasticity and durability to ensure stable electrical properties [83].

Researchers have suggested using fabrics to design and maintain the spacer layer in 3D-structure-based TENGs [84]. Furthermore, the flexibility and breathability of these TENGs are crucial indicators for signal acquisition and skin comfort [31]. This section focuses on the correlation between the developments of spacer layers in 3D-structure-based TENGs, providing valuable insights into the advancement of 3D-structure-based TENGs.

In early studies, attempts were made to improve the rebound in the spacer layer of 3D fabrics by incorporating elastic sponges or additives [56, 57, 85]. However, this approach resulted in bulky 3D-structure-based TENGs, which limited the contact between the friction layers [55, 73]. Additionally, the poor compatibility of the elastic additives and fabric shortened the service lives of TENGs [63].

To address these challenges, Gong et al. [43] designed TENGs based on a fabric geometric structure, with a flexible conductive, dielectric beam, and dielectric layer, using conventional rigid-spring-supported 3D TENGs as a model. As shown in Fig. 11a, the conductive top and dielectric bottom layers consist of different friction materials, whereas the intermediate spacer material comprises a neutral friction material or the same material as the dielectric bottom layer to prevent interference with the conductive top layer. Compared with elastic sponges or additives, a flexible dielectric beam provides a larger spacing, improving the contact and separation between the top and bottom layers and increasing the effective contact area. Figure 11b shows a spacing of approximately 1 mm between the conductive top layer and dielectric bottom layer, resulting in a maximum power density of 1,768.2 mW/m² with an effective area of only 56.7 cm² at a matching resistance of 50 MΩ. Furthermore,

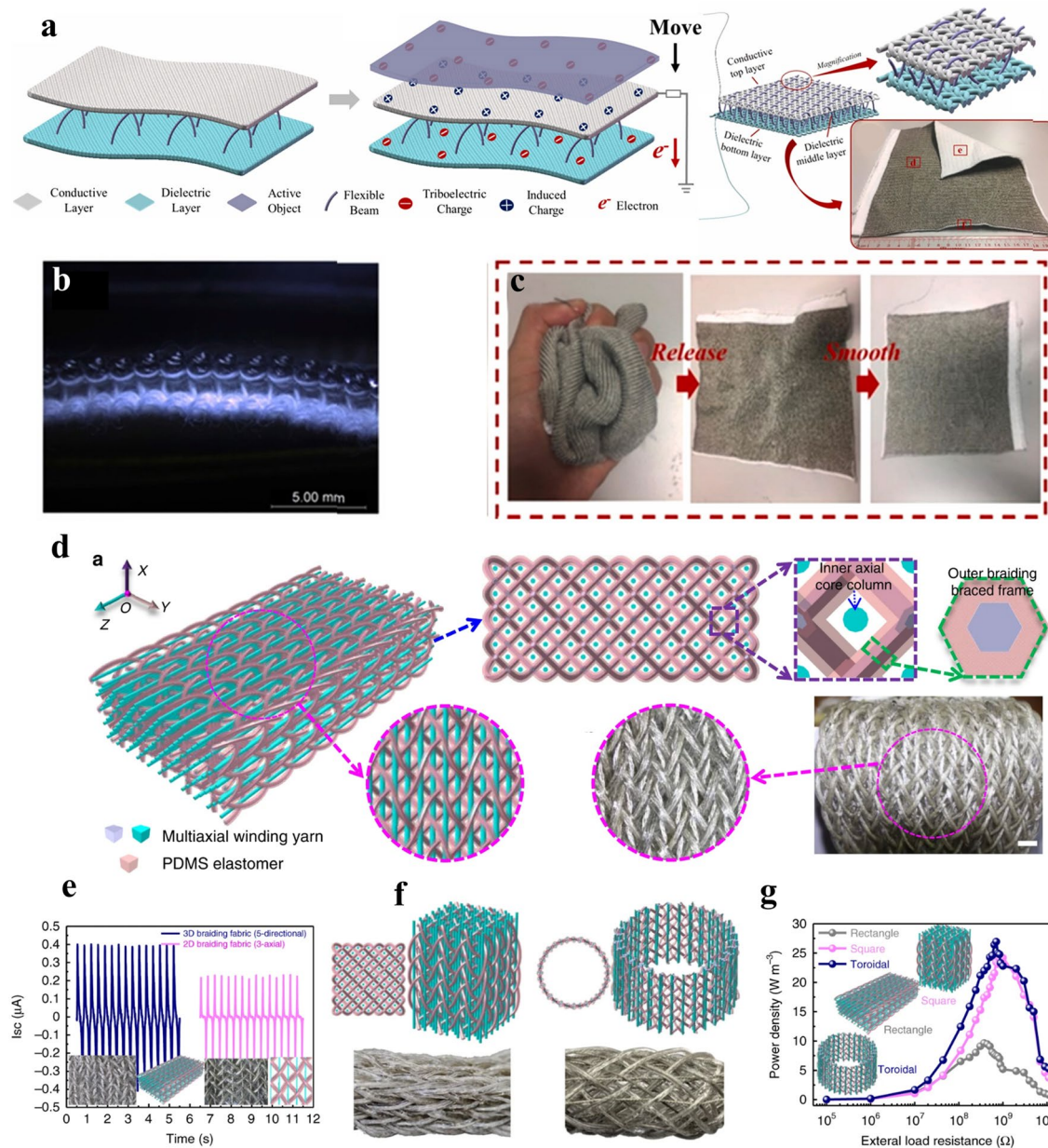


Fig. 11 Flexible fabric geometric TENGs: **a** schematic; **b** dielectric interlayer; **c** ultra-flexibility and wrinkle resistance tests; reproduced with permission from ref [43], Copyright 2019, Elsevier. 3D woven structure TENGs; **d** structural characteristics; **e** electrical output; **f**

comparison of the power densities with rectangular and circular cross sections; **g** comparison of the output power densities of circular and square fabrics; reproduced with permission from ref [44], Copyright 2020, Springer Nature

Fig. 11c shows the ability of the TENG to smoothly recover its original appearance after arbitrary coiling and twisting.

In addition, special 3D braided structures with increased contact–separation spaces have proven to be effective in enhancing the total power output. For instance, Dong et al. developed shape-adaptive and highly elastic woven-structured TENGs based on a 3D five-way braided structure, which created a large contact space owing to the spatial frame structure between the outer braided yarn and inner

axial yarn (Fig. 11d) [44]. The increased contact space resulted in nearly twice the output current compared with a multi-layer 2D TENG fabric of the same size (Fig. 11e). Dong also explored different cross-sectional shapes, such as square and ring shapes, and examined their electrical performance (Fig. 11f). The results indicated that the ring-shaped configuration exhibited a higher output power than the rectangular configuration (Fig. 11g), thus confirming that

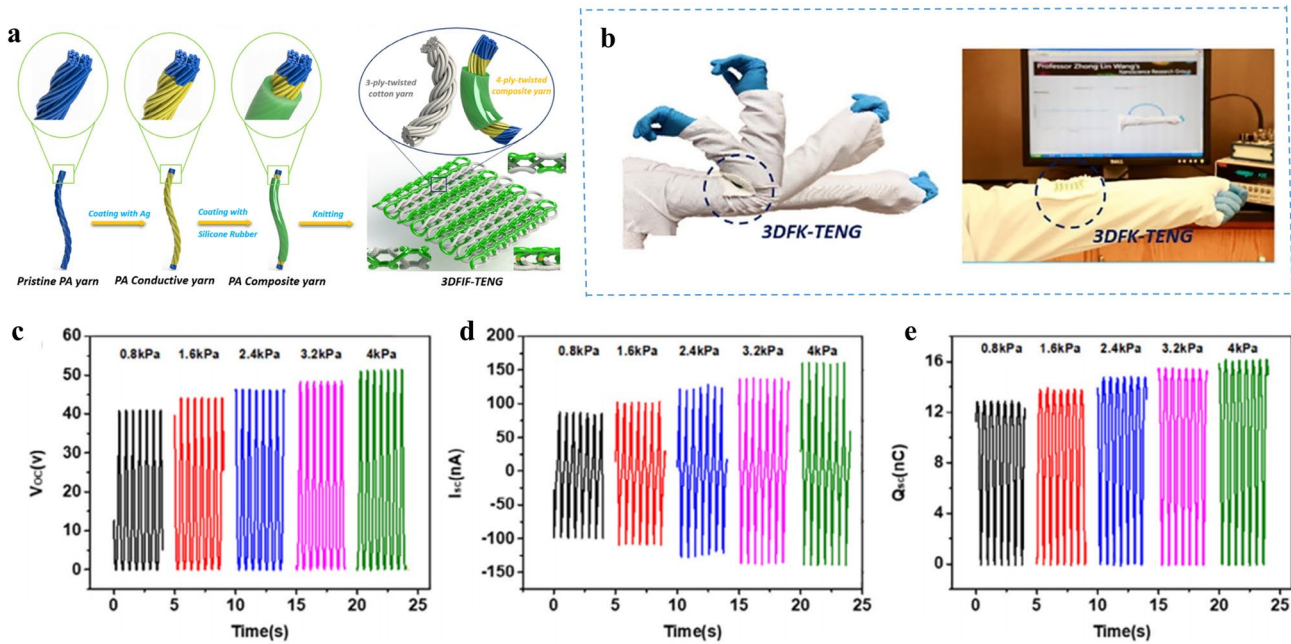


Fig. 12 TENGs for 3D double-sided interlocking fabrics: **a** fabrication process; **b** sensor for detecting arm curvature; **c** voltage, **d** current, and **e** charge output of the fabric with respect to the pressure

during contact separation; Reproduced with permission from ref [12], Copyright 2019, Elsevier

the fabric geometric structure of TENGs, in addition to the friction material, significantly affects their electrical output.

Various designs of spacer layers for 3D-structure-based TENGs have been reported. In addition to using computer programming to design flexible dielectric beams, researchers have employed interlocking structures using 3D fabrics. For example, Chen et al. [12] developed a 3D interlocking structure using a weft-knitted fabric produced with a double-needle-bed flat knitting machine technique for biomotor energy harvesting, self-powered stretching, and haptic sensors. As shown in Fig. 12a, four twisted silver-coated polyamide (PA) yarns were covered with silicone rubber, forming a PA composite yarn. The PA composite yarn and a cotton thread were used as friction materials. When the unique structure of the 3D spacer layer was inserted into the warp and weft, the fabric geometric TENGs gained multifunctional 3D tactile sensor capabilities, allowing the detection of bending in human arms or fingers (Fig. 12b). Furthermore, the voltage, current, and charge exhibited linear increases with an increase in the pressure, making these TENGs suitable for pressure or weight sensors (Fig. 12c–e).

In addition to utilizing various weaving methods to design 3D fabric spacer layers, fabric geometric TENGs can be constructed using different zigzag fabric structures. For example, arch-shaped TENGs (Fig. 13a) [86, 87] can be employed. The height of the arch significantly affects the output of all the electrical properties. The variations in the open-circuit voltage under strain for different arch

heights are shown in Fig. 13b, where the open-circuit voltage becomes linear with the applied strain over a certain range. Thus, TENGs with various arch heights can be used for finger-bend sensing and other applications (Fig. 13c). Figure 13d and e demonstrates the devices for detecting the CO₂ concentration and the curves of the degree of charge-transfer variation with respect to the CO₂ concentration for different friction materials. Wearable fabric-based TENGs are suitable for gas detection because of their good breathability [45].

From the above overview, we see that the TENGs of different dimensions have different structural characteristics and application scenarios, which are summarized in Table 1.

Classification Based on Fabrication Method

Fabric geometric TENGs can be categorized as woven or knitted, depending on their manufacturing and processing methods. The electrical properties of TENGs are significantly affected by their geometric patterns; thus, it is crucial to investigate the effects of different fabrication techniques and geometric structures on the performance of TENGs [92]. This research can provide valuable guidance for optimizing the electrical performance of TENGs.

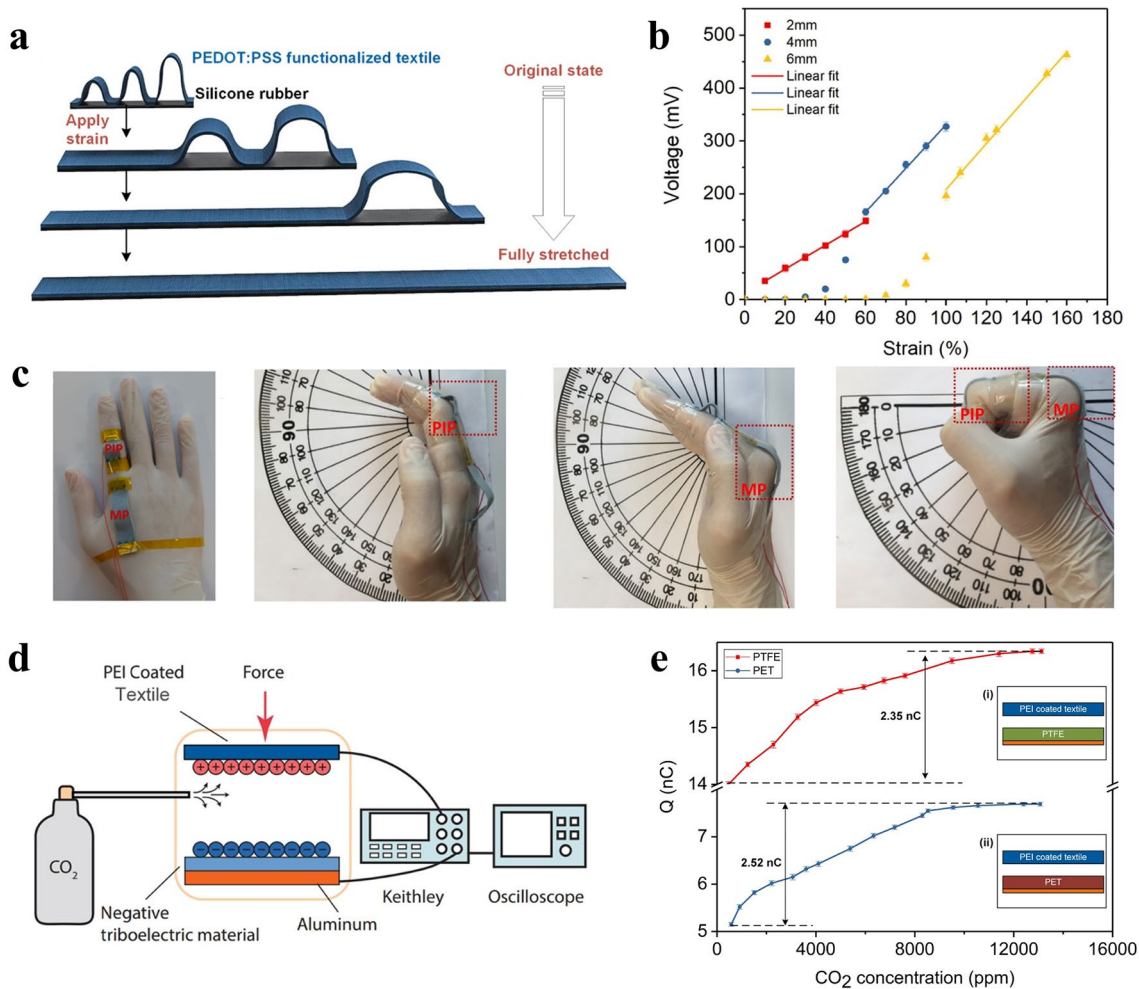


Fig. 13 Arch-shaped TENGs: **a** schematic of the shape change of the arch-shaped sensor; **b** open-circuit voltages with different strains applied for arch heights of 2, 4, and 6 mm; **c** finger-bending sensing at different angles; **d** schematic of CO₂ concentration detection; **e**

response curves of different negative frictional electric materials for charge transfer to the CO₂ concentration; reproduced with permission from ref [45], Copyright 2018, Elsevier

Woven Fabrics (Plain/Twill/Satin)

Woven fabrics are created using interlocking warps and weft yarns in an orthogonal pattern on a loom, with undulating and interlocking structures. These fabrics can be categorized into three basic types: plain (Fig. 14a), twill (Fig. 14b), and satin (Fig. 14c). The importance of different weaves in TENGs was confirmed by Chen et al. (Fig. 14d) [46]. As shown in Fig. 14e, the electrical properties of TENGs formed by interweaving PTFE strips and copper electrodes vary according to the effective contact area. Comparing the outputs of the three basic weaves and the electrical properties of the plain, twill, and satin fabrics reveals that the plain fabrics have the highest electrical output, the twill fabrics have the lowest electrical output, and the satin fabrics fall in between (Fig. 14f). Most 2D fabrics rely on these three basic weaves; however, specific materials can also be

selected to construct TENGs with different weaves for use in various scenarios [93]. For example, woven fabrics with flame-retardant 3D honeycomb structures can be utilized for fire escape and rescue applications [51, 94]. Moreover, combining woven fabrics with waterproof materials allows energy harvesting in severe weather environments [75]. Furthermore, independently woven TENGs with positive and negative alternating all-around sliding energy harvesting have been developed [50], demonstrating the versatility and potential of fabric choices in TENG applications.

Knitted Fabrics

Knitted fabrics are created by interlocking yarns in specific patterns using a knitting machine. There are two primary types of knitted structures: wrap and weft (Fig. 15a and b). TENGs based on fabric geometric structures that utilize

Table 1 Output performance of TENGs with different dimensions

Dimension	Active materials	Electrode	Structure	Electrical outputs	Main applications	Refs.
1D	CCT, PTFF	Carbon nanotubes (CNTs)	Spiral wrap	11.22 nA, 11.08 mW (5 Hz, 9 cm, 2.15% strain)	Medical sensing, health monitoring	[37]
	Silicone rubber	Silver-plated nylon yarn	Coaxial spiral structure	11 W/m ³ (compressed), 0.88 W/m ³ (tensile)	Self-counting rope skipping, gesture recognition, etc	[73]
	Polydimethylsiloxane (PDMS)	Silver nanowires (Ag NWs)/carbon nanotubes (CNTs)	Coaxial structure	22 V, 7.5 nC, 0.6 μA (5 cm, 5 Hz)	Finger-bending sensing and gesture recognition	[88]
	P(VDF-TrFE)	Stretchable electrodes	Fermat spiral structure	105 V, 1.2 μA (30 cm, 2 Hz)	Gesture recognition, water-droplet power generation	[89]
	Polyurethane or spandex	Stainless-steel yarn	Plain weave core-shell yarn	75 V, 1.2 μA(4.5 cm×8 cm)	Biomechanical energy harvesting	[38]
2D	PVDF yarn	Silver-plated nylon yarn	Shell yarn knitting	14.6 V, 4.9 nC, 80.7 nA (3 Hz)	Biomechanical energy harvesting and self-powered sensing	[41]
	PA66, P (VDF-TrFE)	Stainless-steel yarn	Electrostatic spinning	96 V, 8.5 μA (5 cm×5 cm, 200 N, 3 Hz)	Biomechanical energy harvesting and self-powered sensing	[42]
	ZnSnO ₃ /PVDF-HFP nanofibrous films	Aluminum	Coaxial spiral structure	138 V, 5 μA, 52 μC/m ² , 1.6 W/m ²	Harvesting of mechanical energy, e.g., jumping rope	[90]
	Silver-plated nylon fiber, polyacrylonitrile fiber	Silver-plated nylon fiber	Sandwich structure	1,768.2 mW/m ² (50 MΩ, 1200 N)	Biomechanical energy harvesting	[43]
	Polydimethylsiloxane, silver-plated nylon yarns	Silver-plated nylon yarn	Space frame column structure	90 V, 26 W/m ³ (3 Hz, 20 N)	Biomechanical energy harvesting and multifunctional pressure sensing	[44]
3D	Cotton and Nylon 66	Silver-plated polyamide	Double-sided interlocking structure	45 V(5 cm×5 cm, 2 kPa)	Self-powered sensors	[12]
	Polytetrafluoroethylene	Poly(3,4-ethylenedioxythiophene):poly(styrene sulfonate) (PEDOT:PSS) coating, aluminum	Architrave	49.7 V, 787 nA (5 cm×5 cm)	Self-driven sensing and CO ₂ gas detection	[45]
	Silicone rubber	Ti ₃ C ₂ MXene nanosheets	Sandwich structure	400 V, 680 nA	Flexible sensors	[91]
	PDMS/PVDF film, nylon	Cu-Ni cloth	Sandwich structure	600 V, 15 μA, 5.67 W/m ²	Self-driven wearable devices	[48]

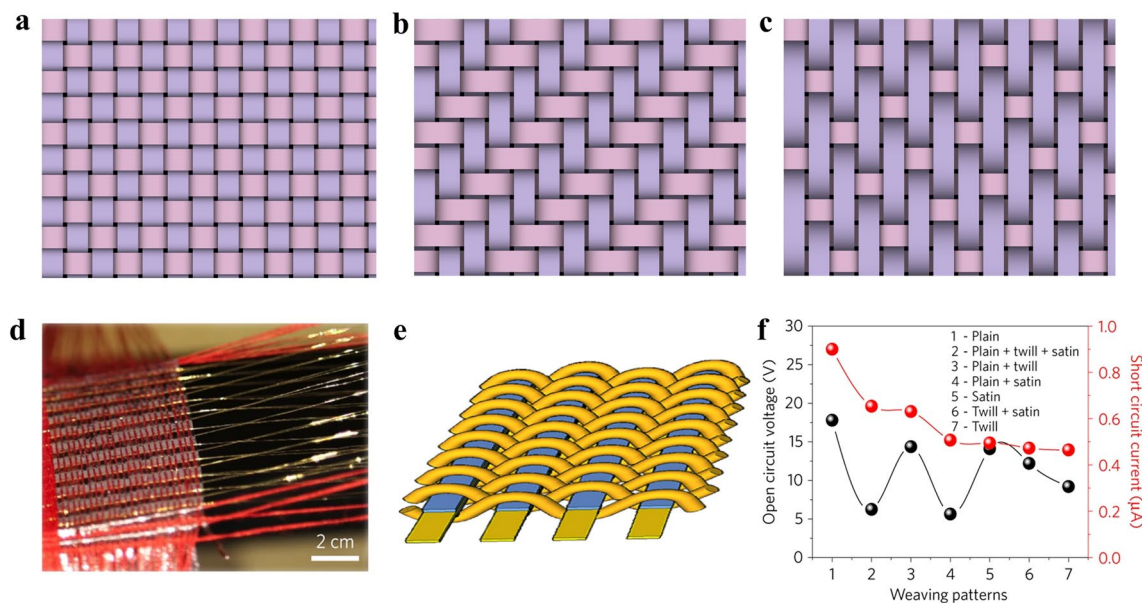


Fig. 14 Woven fabrics: **a** plain tissue; **b** twill tissue; **c** satin tissue. Micro-cable structure woven fabric: **d** photograph of the spinning process; **e** schematic of the structure; **f** output of the electrical properties for different basic tissues; Reproduced with permission from ref [46], Copyright 2016, Springer Nature Limited

ties for different basic tissues; Reproduced with permission from ref [46], Copyright 2016, Springer Nature Limited

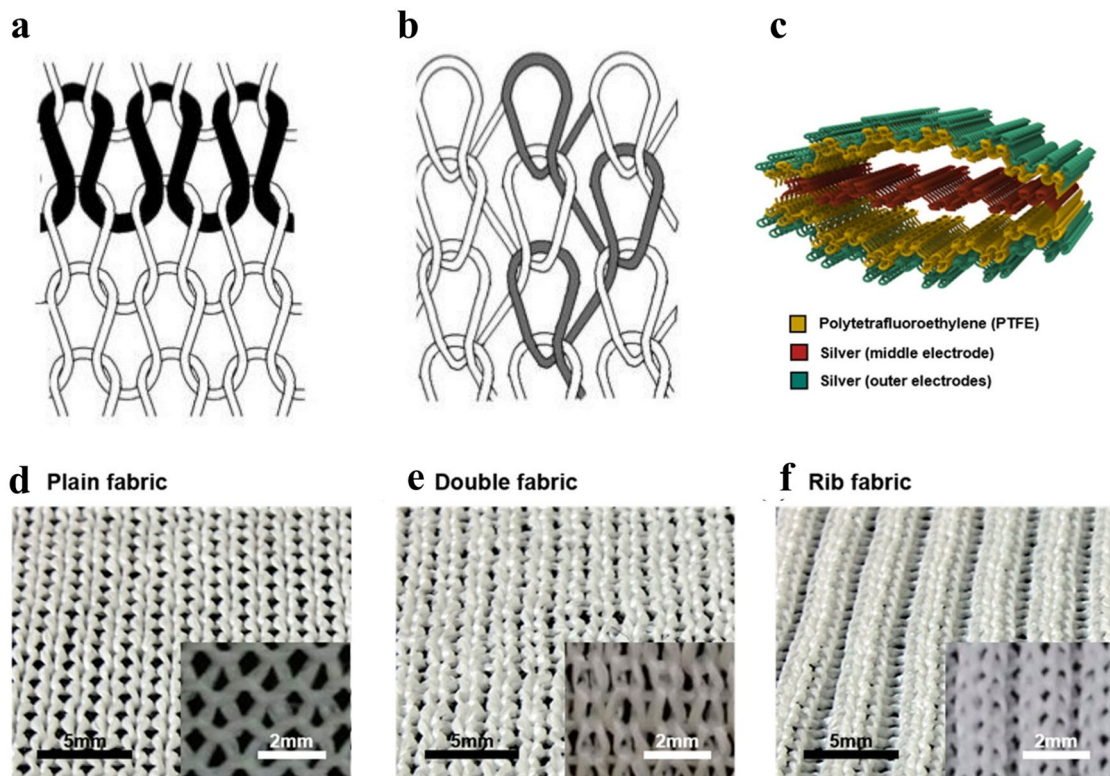


Fig. 15 Knitting fabrics: **a** weft and **b** warp knitting tissues; reproduced with permission from ref [97], Copyright 2017, MDPI. Large deformable knitted structure TENGs: **c** 3D image of the knitted fabric

structure; **d** plain knit structure; **e** double knit structure; **f** ribbed knit structure; reproduced with permission from ref [92], Copyright 2017, American Chemical Society

Table 2 Advantages and disadvantages of TENGs of different dimensions

Classification	Common woven structures	Advantages	Disadvantages
1D	Twisted modified cotton threads [38]	Metal-free and low-cost; easy to integrate with garments	Low output performance The coating material is easily peeled off
	Yarns with a core–shell structure [33, 73]	Structurally stable, can be combined with other elastic fabrics	Time-consuming and complex preparation process
2D	Polymeric film material [98, 99]	Large contact area	Non-washable, non-breathable, and incompatible with fabrics
	Polymer strip materials [42, 100]	Improved washability and breathability	Cross-wound strips limiting the vertical contact–separation distance Strips are susceptible to damage and deformation
	Metal-based electrode fabrics [40, 75]	Weaving from the yarn angle to overcome the disadvantage of easy damage to the strip	Hand-woven and not mechanized Poor flexibility and compatibility
3D	Core–sheath flexible electrodes in tandem with flat fabrics [41]	Soft and comfortable electrodes; strong bonding fastness with fabrics; stable structure, good breathability	High resistance, low current, unable to reach the low-resistance level of metal electrodes
	Core–sheath flexible electrodes in parallel with planar fabrics [42, 79]	Parallel construction for increased current output and enhanced structural stability	Coarse yarn is difficult to weave
	Spacers are elastic sponges, elastic additives, or wavy zigzag structures [56, 57, 85]	Increased triboelectric output from the direction of vertical movement	Poor bonding fastness with fabrics; large overall volume
	The spacer is a flexible axial beam [44]	Large contact area and high output performance	Large overall size makes it difficult to embed into the fabric
	Corrugated multi-arch structures [45]	High stretch	Large volume, one-way stretching only

Table 3 Advantages and disadvantages of common TENG electrodes

Electrodes used for woven-structure-based TENGs	Advantages	Disadvantages
Metal foil (film) [85, 102]	High electrical conductivity	Low tensile strength and air permeability [103]
Metal wires [40, 75]	Flexible and adaptable to textile deformation	Easily fatigued and cracked [79]
Liquid metals and ionic solutions [104]	Deformable and crack-free [77]	Not cuttable, and liquids leak easily [79]
Silver-plated nanowires [102, 105]	Flexible, cuttable, and deformable [110, 111]	High resistance, high cost, and difficult to mass-produce [79]
Organic gels [106–108]		
Carbon-based electrode materials [83, 109]		

knitted designs exhibit excellent tensile properties owing to the inherent deformability of the yarn loops, making them highly resilient [72, 95]. Kwak investigated the effects of different knitted structures on the electrical properties of TENGs, as shown in Fig. 15c [92]. In this study, fully stretchable TENGs with a knitted fabric structure comprising PTFE and silver yarns were developed. The electrode layer was divided into inner and outer silver electrode layers. Under periodic pressure, an alternating current was generated between the inner and outer electrodes. Furthermore, Kwak explored the properties of plain, double, and ribbed structured weft-knitted fabrics and concluded that ribbed fabrics provided larger contact areas and improved tensile

properties (Fig. 15d–f). However, in practical applications, the output of TENGs often lacks stability, resulting in insufficient power for electronic devices with high-power stability requirements. To address this challenge, the integration of energy-storage yarns and energy-harvesting fabrics using weft knitting technology should be considered. This approach will facilitate the preparation of knitted fabrics with a stable output and high elasticity that can be adapted to complex deformations and satisfy the requirements of smart wearables [96]. Furthermore, fabric texture designs can be employed to enhance the performance of knitted TENGs [53].

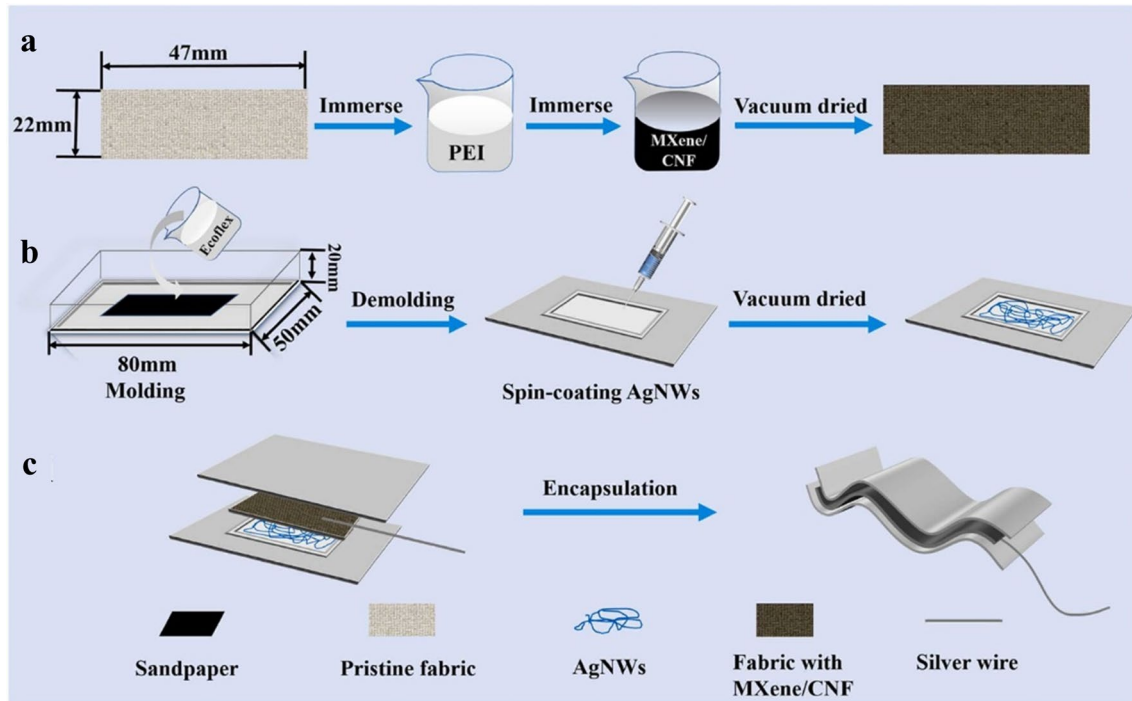


Fig. 16 Schematic of the TENG fabrication process: **a** based on MXene cellulose nanofibers impregnated with cotton fabric to form the electrode layer, **b** using liquid silicone rubber to form the friction

layer, and **c** involving two friction layers and one electrode layer encapsulated into a TENG; reproduced with permission from ref [91], Copyright 2022, Elsevier

Optimization of Performance of Fabric Geometric TENGs

Advantages and Disadvantages of TENGs of Different Dimensions

Wearable electronic devices have considerable potential for integration with textiles, potentially allowing the harmonious combination of device functionality with the softness, breathability, and comfort of the fabric [33]. For example, wearable electronic devices can help track vital signs and monitor fitness activities [11, 12]. Additionally, the energy supply for wearable electronic devices is closely related to advancements in fabric geometric TENG research. Fabric geometric TENGs offer an eco-friendly approach to energy harvesting. The fabric geometric structure significantly affects the electrical properties of TENGs for a specific friction material. Moreover, researchers have studied the effects of fabrication techniques on the electrical properties of various textile molding methods. Table 2 presents a comprehensive overview of the advantages and disadvantages of different types of fabric geometric TENGs.

TENGs Based on Composites and Surface-Modified Fabric

Fabric geometric TENGs that combine TENG technology with traditional textile techniques offer promising opportunities for bioenergy harvesting and powering wearable electronic devices, as well as enhancing comfort and integration with the human body. However, compared with rigid structural materials or polymers, textile materials inherently have a limited capacity to gain or lose electrons on their surfaces, resulting in a lower frictional charge density [43]. Furthermore, in the case of fabric geometric TENGs, the electrodes must be compatible with the softness, breathability, and comfort of the fabric. The insufficient bonding strength between the electrodes and fabric can impact charge collection and subsequently affect the output of TENGs. Thus, there are substantial challenges in selecting suitable electrodes and ensuring strong electrode-to-fabric bonding [101]. Table 3 summarizes the advantages and disadvantages associated with common electrodes used in fabric geometric TENGs.

To enhance the capabilities of capturing and releasing electrons on the surfaces of materials and address the issue of poor bonding between electrodes and fabrics, researchers have proposed composite approaches that combine polymers with fabrics through fabric modification methods [112–114],

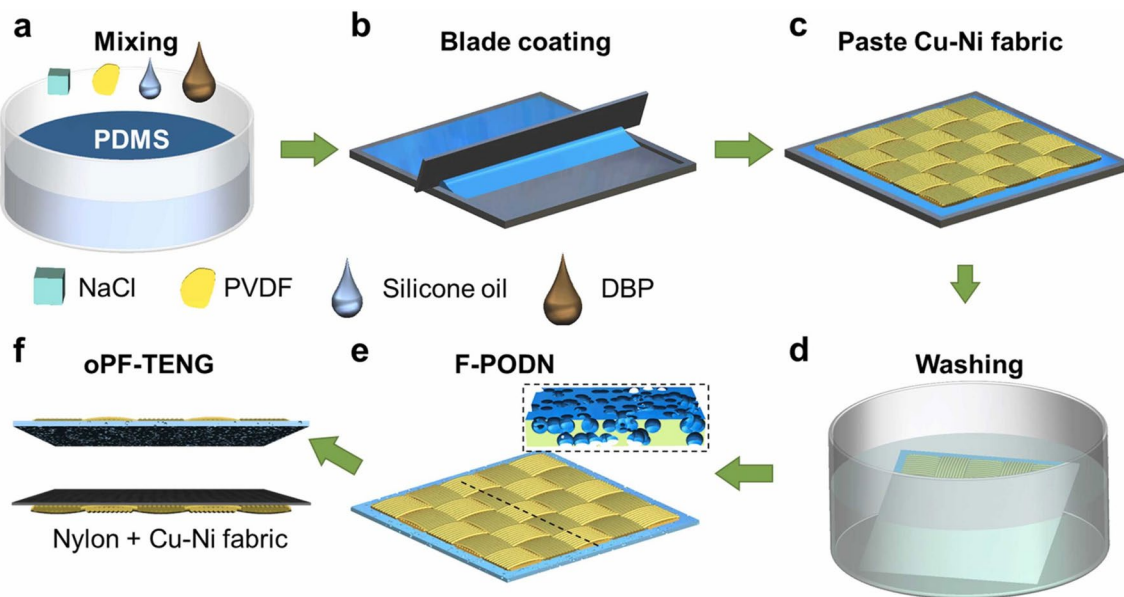


Fig. 17 Fabrication process for porous breathable fabrics: **a** mixing of PDMS, NaCl particles, dibutyl phthalate (DBP), silicone oil, and PVDF powder; **b** blades of the mixture are coated; **c** adhesion of CuNi cloth as a back electrode and curing; **d** washing to remove DBP,

silicone oil, and NaCl particles; **e** drying to obtain an open-pore film; **f** porous breathable fabric TENGs; reproduced with permission from ref [48], Copyright 2022, Elsevier

such as impregnation and coating techniques. Impregnation is a simple and effective method for fabricating polymer-wrapped fabric composites [91]. In contrast, surface coating involves applying a polymer coating onto the fabric surface, which allows the inherent properties of the fabric to be fully retained [48, 115]. Furthermore, functional TENGs can be created by modifying the fabric surface to achieve waterproofing by altering the hydrophobicity of the fabric [116]. These advancements have resulted in increased development of versatile TENGs with enhanced performance and tailored functionalities.

Figure 16a illustrates the fabricating process of highly conductive electrodes by immersing cotton fabric in a solution of MXene and cellulose nanofibers. These electrodes, combined with the rubber material presented in Fig. 16b, form TENGs that function as self-powered flexible sensors (Fig. 16c). The cotton fabric serves as a sturdy and flexible base for the electrode layer, while the electronegativity provided by Ti_3C_2 MXene on the electrode's surface contributes to its conductivity. This configuration allows the generation of a high open-circuit voltage of up to 400 V in the single-electrode mode [91].

Tan proposed that most textile materials, such as cotton, silk, and nylon, have positive frictional electrode properties. However, there is a greater need for negatively charged textile materials or materials coated with a negative polarity. Thus, Tan developed a TENG using a breathable fabric as the negative electrode material; the TENG was coated with PDMS, which has a porous structure

[48]. The open porous structure had a permeability of 73 mm/s, overcoming the limitations of impermeable coating structures. Furthermore, the porous structure and the addition of the PVDF filler significantly enhanced the frictional electrical output. The resulting TENGs, which had a woven structure and measured $4 \times 4 \text{ cm}^2$, achieved an open-circuit voltage of 600 V, a short-circuit current of 15 μA , and a power density of 5.67 W/m^2 . Figure 17 illustrates the process that utilizes PDMS, silicone oil, dibutyl phthalate, and sodium chloride microparticles as pore-forming agents. The final TENGs are obtained after coating, curing, washing, and drying.

Conclusions and Perspectives

Conclusions

In this review, we comprehensively considered the relationship between the electrode and friction material of fabric geometric TENGs rather than relying on their electrical output as the only criterion for evaluation. Moreover, we examined TENGs with different dimensions and weaving styles.

In 1D yarn-based TENGs, which have a relatively limited range of applications and low output performance, textiles are mostly used as carriers [117, 118] (refer to Table 1). Weaving yarns into 2D or 3D structures has proven to be a more favorable method for harvesting

human kinetic energy. 2D-structure-based TENGs, which employ textiles for sensing applications and can collect mechanical energy in non-vertical motion directions, are promising in the field of self-powered sensing. Furthermore, 3D-structure-based TENGs primarily designed for vertical motion are well suited for bioenergy harvesting—particularly in the context of human motion, where vertical motion dominates. Nonetheless, it is essential to consider the inherent volume of 3D structures and their integration into fabrics to address the challenges related to resilience and other associated factors. A clear design of the relationship between friction and spacer layers to capture both the vertical and horizontal motions of fabric geometric structures can lead to a larger market and a wider range of applications [86].

Although TENGs based on composite materials and surface modifications can overcome the issue of low inherent frictional charges in materials, they have disadvantages. For instance, combining polymers with fabrics tends to reduce their flexibility, air permeability, and tensile strength, while the impregnation method may damage the fabric, as the preparation time is long and the process is complex and expensive [74]. Although the coating method or surface modification allows better retention of material properties, the non-uniformity of the fabric surface may result in defects in the coating, which can affect the stability of the fabric [91]. Additionally, the gradual peeling

of the coated material with repeated washing needs to be addressed [41].

To summarize the characteristics of the aforementioned fabric geometric TENGs, we can selectively choose TENGs compatible with the equipment's function according to different environments and apply them to various scenarios by carefully selecting friction materials, designing appropriate structures, and utilizing surface modification techniques. For instance, using materials with opposite polarities, such as polyimides with high-temperature resistance and wool with high-temperature heat shrinkage, can result in distinct rebound properties in hot and humid environments. Flame-retardant conductive cotton fabrics can be employed to develop fabric geometric TENGs for fire-related applications [51, 94]. Surface modification techniques can be utilized to impart hydrophobicity to fabric surfaces, making them suitable for use in severe weather conditions and underwater sensing [48, 119]. Additionally, acid- and alkali-resistant woven-structure TENGs can provide intelligent protection for self-powered monitoring of liquid energy harvesting in high-risk environments [54, 120]. However, in applications in different scenarios, the impact of comfort, breathability, wash durability, temperature, and humidity on fabric geometric TENGs is often overlooked [115, 121].

Studies have indicated that the electrical properties of TENGs tend to deteriorate with increasing temperature and humidity. High temperatures can reduce the charge on the

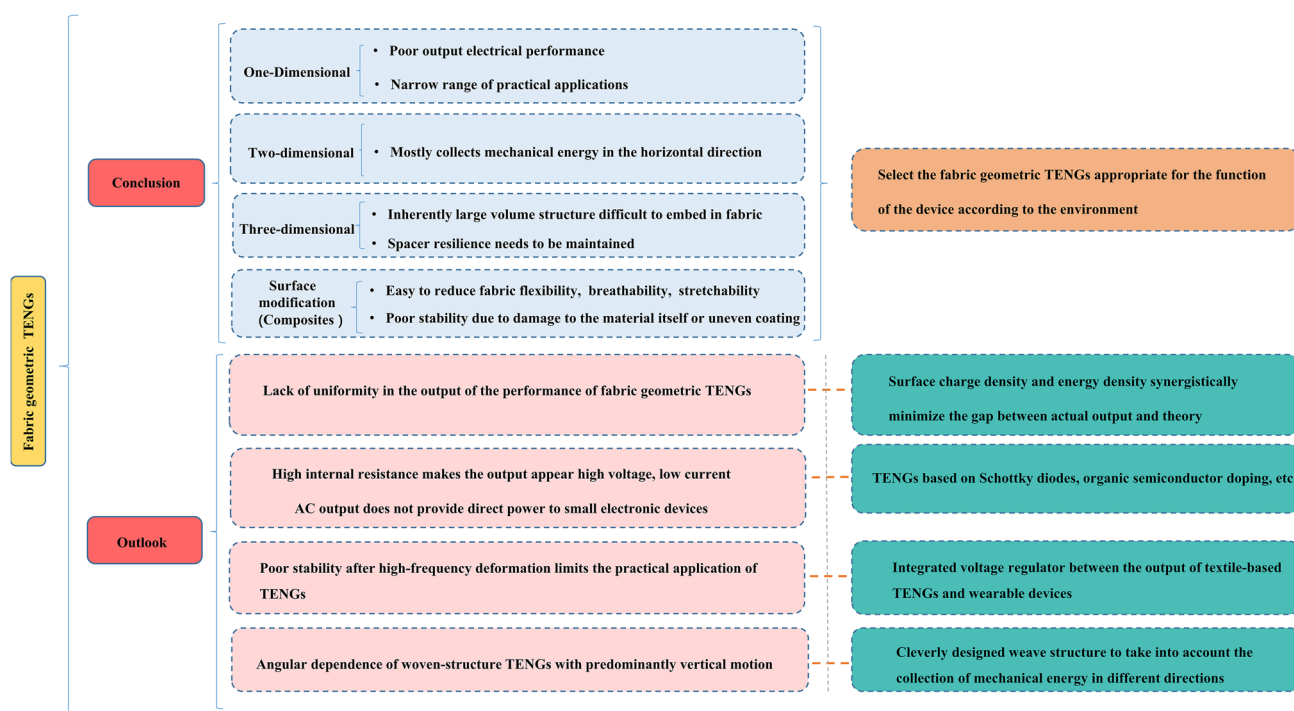


Fig. 18 Conclusions and outlook regarding fabric geometric TENGs

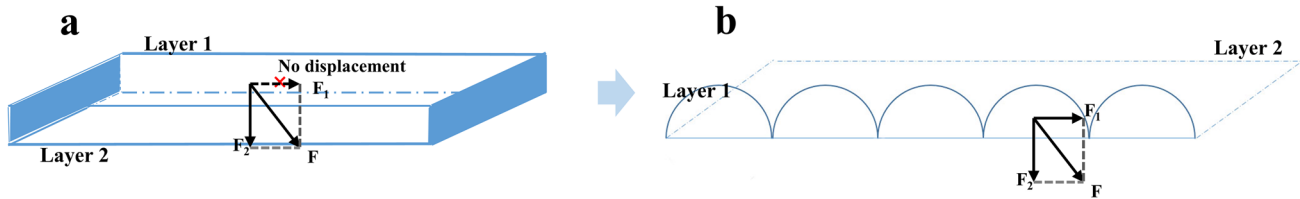


Fig. 19 Schematic of the fabric geometric TENGs without angular dependence

surface of a friction material, whereas moisture in the environment tends to be adsorbed onto the surface of the friction material, impeding charge transfer between the contacting surfaces [122, 123]. Therefore, it is crucial to consider these factors and their effects when designing and utilizing fabric geometric TENGs.

Perspective

Current Opportunities and Challenges of Fabric Geometric TENGs

The output performance of the fabric geometric TENGs exhibits a lack of uniformity. Various parameters, including the area and external resistance, contribute in different ways to the overall output performance of TENGs. These parameters significantly affect the electrical properties. Notably, the intrinsic output performance of the TENGs in the vertical-separation mode is derived from electrodynamics as follows:

$$VOC = \frac{\sigma h(t)}{\epsilon_0} \quad (1)$$

$$C = \frac{\epsilon_0 S}{d_0 + h(t)} \quad (2)$$

$$QSC = \frac{S \sigma h(t)}{d_0 + h(t)}, \quad (3)$$

where ϵ_0 means dielectric constant of vacuum; σ means surface charge density; d_0 means ratio of dielectric material thickness between the electrodes to their respective dielectric constants; $h(t)$ means average separation distance of the two friction materials; S means effective contact area of the friction material.

However, measuring the output performance of TENGs in a standardized manner continues to pose challenges [57]. Although surface charge density has been suggested as a measure of TENG performance, it is sensitive to external factors such as temperature, humidity, and atmospheric pressure. Thus, the intrinsic frictional electricity of a material cannot be directly characterized [1]. For instance, Liu

emphasized that the surface charge density, which is affected by factors such as the polarity of the friction material, surface roughness, and effective contact area, is a key factor in measuring performance parameters such as the output voltage, current, and power density [93]. Zhou et al. introduced energy density as a measure to represent the area enclosed by voltage and charge, examining over 40 materials to assess the effects of the atmospheric pressure, temperature, humidity, thickness, and area on frictional charge density, intending to minimize the gap between the actual and theoretical maximum output performance [124].

Currently, fabric geometric TENGs exhibit high internal resistance, leading to a high voltage and low current output, posing a challenge for directly driving low-resistance electronic devices in everyday life, because impedance balancing requires load resistance within the measurement range. Moreover, the AC output of fabric geometric TENGs cannot directly power small electronic devices [125] and requires rectification. The traditional rectifier devices consist of four diodes, which are large and incompatible with fabrics. Therefore, it would be beneficial to enhance their integration and seamlessly combine them with fabric geometric TENGs without compromising the inherent characteristics of the fabric. Researchers have reported using Schottky diodes to directly convert mechanical forces into direct-current power or enhance the electrical performance of TENGs via doping organic semiconductors and excitation of electron–hole pairs [126, 127]. Although the preparation process is intricate, these approaches provide valuable insights for advancing the development of fabric geometric TENGs. In addition, most woven-structure TENGs exhibit transient and unstable voltage characteristics. To address this issue, researchers have integrated energy-storage circuits into fabrics, along with TENGs. However, the conventional size and rigidity of capacitors make their integration into fabrics challenging. Therefore, enhancing capacitor integration or developing flexible capacitors to combine with fabric geometric TENGs is a promising research direction. By addressing the challenges related to the impedance mismatch between TENGs and electronic devices, the development prospects of fabric geometric TENGs for powering wearable devices, bioenergy harvesting, and sensing can be considerably broadened (Fig. 18).

According to the comprehensive review, researchers have successfully developed 2D fabric geometric TENGs capable of collecting energy in multiple directions, addressing the limitation of TENGs only collecting energy in one direction [50]. However, most TENGs based on a 3D fabric geometry have angular dependence when collecting energy in the vertical direction of human motion. Therefore, there is an urgent need for textile-based TENGs without angular dependence that can collect mechanical energy in different directions. In particular, for the fabric geometric TENGs with biplane electrode materials, only the induced charge generated by the displacement change in the vertical direction (F_2) can convert the mechanical energy of that direction into electrical energy, with the mechanical energy exerted by the horizontal component (F_1) of the force often wasted (Fig. 19a). To solve this problem, we propose a fabric geometric TENG with a ‘bulging bag’ structure. The bulging bag can decompose the force exerted in any direction into forces in the tangential (F_1) and normal (F_2) directions of the fabric, which allows the fabric to generate displacements in both the normal and tangential directions, allowing the utilization of mechanical energy in both directions. Hence, mechanical energy can be collected in all directions without angular dependence, thus providing new insight into the future development of 3D woven-structure TENGs with a high friction electric output (Fig. 19b).

Future Applications of Fabric Geometric TENGs

Smart medicine: Using fabric geometric TENGs, self-driven sensing can be achieved for Internet medical treatment and human health and safety detection, possibly leading to more accurate, data-oriented, and scientific medical diagnosis. For example, a self-driven human motion-sensing network integrating multiple fabrics can collect multichannel signals of human motion in real time. Through this network, effective multipoint detection of whole-body gait information can be achieved, thus providing a promising solution for clinical diagnosis and rehabilitation assistance for conditions such as Parkinson’s disease and scissor gait [128].

Intelligent clothing: As clothing is essential for the human body and remains closely attached to it, smart clothing constructed using fibers or fabrics has unique advantages for harvesting biomechanical energy from the human body and self-powered sensing. Through fabric weaving, it can dynamically sense and balance the regulation of the human body to adapt to the external environment, which is of considerable importance. For example, firefighting clothing prepared using conductive aerogel fibers can withstand temperatures between 100 and 400 °C and also be used for self-powered fire localization, providing good fire warning capabilities [129]. Moreover, smart clothes can power wearable small electronic devices that

combine the softness and breathability of clothing with washability, durability, etc., while collecting energy from various movement modes.

Smart applications: Advancements in the Internet of Things, artificial intelligence, and distributed networks will allow human–computer interaction through smart textiles. This innovation allows machines to easily sense electrical signals from external stimuli, understand various human commands, and provide feedback. Combining fabric geometric TENGs with artificial intelligence can result in more accurate recognition of signals. For instance, Ma et al. designed a smart carpet with a 3D honeycomb structure that guides people to find the correct escape route in extreme fire environments [130]. Utilizing machine learning alongside smart carpets allows accurate recognition of the human body based on gait patterns and facilitates human–machine interaction. Moreover, it is possible to design fabric geometric TENGs using all-fiber flexible materials and create self-powered wearable human–computer interaction keyboards through a combination of flexible and stretchable textiles and self-powered sensing [131].

Acknowledgements The authors are thankful for financial support from the National Natural Science Foundation of China (U21A2095) and the Key Research and Development Program of Hubei Province (2021BAA068).

Data availability Data availability is not applicable to this article as no new data were created or analyzed in this study.

Declarations

Conflict of Interest The authors declare that there is no conflict of interest regarding the publication of this article.

References

- Chi JG, Liu CR, Che LF, Li DJ, Fan K, Li Q, Yang WH, Dong LX, Wang GF, Wang ZL. Harvesting water-evaporation-induced electricity based on liquid-solid triboelectric nanogenerator. *Adv Sci*. 2022;9:2201586.
- Dan XZ, Cao R, Cao XL, Wang YF, Xiong Y, Han J, Luo L, Yang JH, Xu N, Sun J, Sun QJ, Wang ZL. Whirligig-inspired hybrid nanogenerator for multi-strategy energy harvesting. *Adv Fiber Mater*. 2023;5:362.
- Dudem B, Kim DH, Yu JS. Triboelectric nanogenerators with gold-thin-film-coated conductive textile as floating electrode for scavenging wind energy. *Nano Res*. 2018;11:101.
- Wu YC, Zhong XD, Wang X, Yang Y, Wang ZL. Hybrid energy cell for simultaneously harvesting wind, solar, and chemical energies. *Nano Res*. 2014;7:1631.
- Yang Y, Zhu G, Zhang HL, Chen J, Zhong XD, Lin ZH, Su YJ, Bai P, Wen XN, Wang ZL. Triboelectric nanogenerator for harvesting wind energy and as self-powered wind vector sensor system. *ACS Nano*. 2013;7:9461.
- Zhang L, Zhang BB, Chen J, Jin L, Deng WL, Tang JF, Zhang HT, Pan H, Zhu MH, Yang WQ, Wang ZL. Lawn structured

- triboelectric nanogenerators for scavenging sweeping wind energy on rooftops. *Adv Mater.* **2016**;28:1650.
7. Jiang T, Zhang LM, Chen XY, Han CB, Tang W, Zhang C, Xu L, Wang ZL. Structural optimization of triboelectric nanogenerator for harvesting water wave energy. *ACS Nano.* **2015**;9:12562.
 8. Jiang T, Yao YY, Xu L, Zhang LM, Xiao TX, Wang ZL. Spring-assisted triboelectric nanogenerator for efficiently harvesting water wave energy. *Nano Energy.* **2017**;31:560.
 9. Xiong JQ, Lin MF, Wang JX, Gaw SL, Parida K, Lee PS. Wearable all-fabric-based triboelectric generator for water energy harvesting. *Adv Energy Mater.* **2017**;7:1701243.
 10. Feng JR, Zhou HL, Cao Z, Zhang EY, Xu SX, Li WT, Yao HL, Wan LY, Liu GL. 0.5 m triboelectric nanogenerator for efficient blue energy harvesting of all-sea areas. *Adv Sci.* **2022**;9:2204407.
 11. Luo JJ, Wang ZM, Xu L, Wang AC, Han K, Jiang T, Lai QS, Bai Y, Tang W, Fan FR, Wang ZL. Flexible and durable wood-based triboelectric nanogenerators for self-powered sensing in athletic big data analytics. *Nat Commun.* **2019**;10:5147.
 12. Chen CY, Chen LJ, Wu ZY, Guo HY, Yu WD, Du ZQ, Wang ZL. 3d double-faced interlock fabric triboelectric nanogenerator for bio-motion energy harvesting and as self-powered stretching and 3d tactile sensors. *Mater Today.* **2020**;32:84.
 13. Huo ZY, Kim Y-J, Suh I-Y, Lee D-M, Lee JH, Du Y, Wang S, Yoon H-J, Kim S-W. Triboelectrification induced self-powered microbial disinfection using nanowire-enhanced localized electric field. *Nat Commun.* **2021**;12:3693.
 14. Li JC, Yin J, Wee MGV, Chinnappan A, Ramakrishna S. A self-powered piezoelectric nanofibrous membrane as wearable tactile sensor for human body motion monitoring and recognition. *Adv Fiber Mater.* **2023**. <https://doi.org/10.1007/s42765-023-00282-8>.
 15. You AM, Zhang XL, Peng X, Dong K, Lu YY, Zhang Q. A skin-inspired triboelectric nanogenerator with an interpenetrating structure for motion sensing and energy harvesting. *Macromol Mater Eng.* **2021**;306:2170028.
 16. Dong K, Deng JN, Zi YL, Wang YC, Xu C, Zou HY, Ding WB, Dai YJ, Gu BH, Sun BZ, Wang ZL. 3d orthogonal woven triboelectric nanogenerator for effective biomechanical energy harvesting and as self-powered active motion sensors. *Adv Mater.* **2017**;29:1702648.
 17. He TYY, Sun ZD, Shi QF, Zhu ML, Anaya DV, Xu MY, Chen T, Yuce MR, Thean AV-Y, Lee C. Self-powered glove-based intuitive interface for diversified control applications in real/cyber space. *Nano Energy.* **2019**;58:641.
 18. Zhang CX, Dai KR, Liu D, Yi F, Wang XF, Zhu LQ, You Z. Ultralow quiescent power-consumption wake-up technology based on the bionic triboelectric nanogenerator. *Adv Sci.* **2020**;7:2000254.
 19. Chou S-H, Lu HW, Liu T-C, Chen YT, Fu YL, Shieh Y-H, Lai Y-C, Chen SY. An environmental-inert and highly self-healable elastomer obtained via double-terminal aromatic disulfide design and zwitterionic crosslinked network for use as a triboelectric nanogenerator. *Adv Sci.* **2023**;10:2202815.
 20. Imani IM, Kim B, Xiao X, Rubab N, Park B-J, Kim Y-J, Zhao P, Kang M, Kim S-W. Ultrasound-driven on-demand transient triboelectric nanogenerator for subcutaneous antibacterial activity. *Adv Sci.* **2023**;10:2204801.
 21. Cheedarala RK, Duy LC, Ahn KK. Double characteristic bno-spi-tengs for robust contact electrification by vertical contact separation mode through ion and electron charge transfer. *Nano Energy.* **2018**;44:430.
 22. Parida K, Thangavel G, Cai GF, Zhou XR, Park S, Xiong JQ, Lee PS. Extremely stretchable and self-healing conductor based on thermoplastic elastomer for all-three-dimensional printed triboelectric nanogenerator. *Nat Commun.* **2019**;10:2158.
 23. Wang HM, Xu L, Bai Y, Wang ZL. Pumping up the charge density of a triboelectric nanogenerator by charge-shuttling. *Nat Commun.* **2020**;11:4203.
 24. Niu SM, Liu Y, Wang SH, Lin L, Zhou YS, Hu YF, Wang ZL. Theory of sliding-mode triboelectric nanogenerators. *Adv Mater.* **2013**;25:6184.
 25. Jin T, Sun ZD, Li L, Zhang Q, Zhu ML, Zhang ZX, Yuan GJ, Chen T, Tian YZ, Hou XY, Lee C. Triboelectric nanogenerator sensors for soft robotics aiming at digital twin applications. *Nat Commun.* **2020**;11:5381.
 26. He WC, Liu WL, Chen J, Wang Z, Liu YK, Pu XJ, Yang HM, Tang Q, Yang HK, Guo HY, Hu CG. Boosting output performance of sliding mode triboelectric nanogenerator by charge space-accumulation effect. *Nat Commun.* **2020**;11:4277.
 27. Jurado UT, Pu SH, White NM. Wave impact energy harvesting through water-dielectric triboelectrification with single-electrode triboelectric nanogenerators for battery-less systems. *Nano Energy.* **2020**;78: 105204.
 28. Yu JR, Gao GY, Huang JR, Yang XX, Han J, Zhang H, Chen YH, Zhao CL, Sun QJ, Wang ZL. Contact-electrification-activated artificial afferents at femtojoule energy. *Nat Commun.* **2021**;12:1581.
 29. Shi QF, Lee C. Self-powered bio-inspired spider-net-coding interface using single-electrode triboelectric nanogenerator. *Adv Sci.* **2019**;6:1900617.
 30. Zhang Q, Zhang ZX, Liang QJ, Shi QF, Zhu ML, Lee C. All in one, self-powered bionic artificial nerve based on a triboelectric nanogenerator. *Adv Sci.* **2021**;8:2004727.
 31. Niu SM, Liu Y, Chen XY, Wang SH, Zhou YS, Lin L, Xie YN, Wang ZL. Theory of freestanding triboelectric-layer-based nanogenerators. *Nano Energy.* **2015**;12:760.
 32. So MY, Xu BG, Li ZH, Lai CL, Jiang CHZ. Flexible corrugated triboelectric nanogenerators for efficient biomechanical energy harvesting and human motion monitoring. *Nano Energy.* **2023**;106: 108033.
 33. Lai Y-C, Deng JN, Zhang SL, Niu SM, Guo HY, Wang ZL. Single-thread-based wearable and highly stretchable triboelectric nanogenerators and their applications in cloth-based self-powered human-interactive and biomedical sensing. *Adv Funct Mater.* **2017**;27:1604462.
 34. Yang Y, Chen L, He J, Hou XJ, Qiao XJ, Xiong JJ, Chou XJ. Flexible and extendable honeycomb-shaped triboelectric nanogenerator for effective human motion energy harvesting and biomechanical sensing. *Adv Mater Technol.* **2022**;7:2100702.
 35. Liu X, Liu YZ, Cheng TH, Gao YF, Yang ZQ. A high performing piezoelectric and triboelectric nanogenerator based on a large deformation of the novel lantern-shaped structure. *Nano Energy.* **2022**;92: 106699.
 36. Shi QW, Sun JQ, Hou CY, Li YG, Zhang QH, Wang HZ. Advanced functional fiber and smart textile. *Adv Fiber Mater.* **2019**;1:3.
 37. Zhong JW, Zhang Y, Zhong QZ, Hu QY, Hu B, Wang ZL, Zhou J. Fiber-based generator for wearable electronics and mobile medication. *ACS Nano.* **2014**;8:6273.
 38. Yu AF, Pu X, Wen RM, Liu MM, Zhou T, Zhang K, Zhang Y, Zhai JY, Hu WG, Wang ZL. Core-shell-yarn-based triboelectric nanogenerator textiles as power cloths. *ACS Nano.* **2017**;11:12764.
 39. Pu X, Li LX, Song HQ, Du CH, Zhao ZF, Jiang CY, Cao GZ, Hu WG, Wang ZL. A self-charging power unit by integration of a textile triboelectric nanogenerator and a flexible lithium-ion battery for wearable electronics. *Adv Mater.* **2015**;27:2472.
 40. Ning C, Tian L, Zhao XY, Xiang SX, Tang YJ, Liang E, Mao YC. Washable textile-structured single-electrode triboelectric nanogenerator for self-powered wearable electronics. *J Mater Chem A.* **2018**;6:19143.

41. Li YY, Zhang YH, Yi J, Peng X, Cheng RW, Ning C, Sheng FF, Wang S, Dong K, Wang ZL. Large-scale fabrication of core-shell triboelectric braided fibers and power textiles for energy harvesting and plantar pressure monitoring. *EcoMat.* **2022**;4: e12191.
42. Guan XY, Xu BG, Wu MJ, Jing TT, Yang YJ, Gao YY. Breathable, washable and wearable woven-structured triboelectric nanogenerators utilizing electrospun nanofibers for biomechanical energy harvesting and self-powered sensing. *Nano Energy.* **2021**;80: 105549.
43. Gong JL, Xu BG, Guan XY, Chen YJ, Li SY, Feng J. Towards truly wearable energy harvesters with full structural integrity of fiber materials. *Nano Energy.* **2019**;58:365.
44. Dong K, Peng X, An J, Wang AC, Luo JJ, Sun BZ, Wang J, Wang ZL. Shape adaptable and highly resilient 3d braided triboelectric nanogenerators as e-textiles for power and sensing. *Nat Commun.* **2020**;11:2868.
45. He TYY, Shi QF, Wang H, Wen F, Chen T, Ouyang J, Lee C. Beyond energy harvesting—multi-functional triboelectric nanosensors on a textile. *Nano Energy.* **2019**;57:338.
46. Chen J, Huang Y, Zhang NN, Zou HY, Liu RY, Tao CY, Fan X, Wang ZL. Micro-cable structured textile for simultaneously harvesting solar and mechanical energy. *Nat Energy.* **2016**;1:16138.
47. Rezaei J, Nikfarjam A. Rib stitch knitted extremely stretchable and washable textile triboelectric nanogenerator. *Adv Mater Technol.* **2021**;6:2000983.
48. Tan D, Xu BG, Gao YY, Tang Y, Liu YF, Yang YJ, Li ZH. Breathable fabric-based triboelectric nanogenerators with open-porous architected polydimethylsiloxane coating for wearable applications. *Nano Energy.* **2022**;104: 107873.
49. Lee S, Ko W, Oh Y, Lee J, Baek G, Lee Y, Sohn J, Cha S, Kim J, Park J, Hong J. Triboelectric energy harvester based on wearable textile platforms employing various surface morphologies. *Nano Energy.* **2015**;12:410.
50. Paosangthong W, Wagih M, Torah R, Beeby S. Textile-based triboelectric nanogenerator with alternating positive and negative freestanding woven structure for harvesting sliding energy in all directions. *Nano Energy.* **2022**;92: 106739.
51. Ma LY, Wu RH, Liu S, Patil A, Gong H, Yi J, Sheng FF, Zhang YZ, Wang J, Wang J, Guo WX, Wang ZL. A machine-fabricated 3d honeycomb-structured flame-retardant triboelectric fabric for fire escape and rescue. *Adv Mater.* **2020**;32:2003897.
52. Rahman MT, Rana SMS, Salauddin M, Zahed MA, Lee S, Yoon E-S, Park JY. Silicone-incorporated nanoporous cobalt oxide and mxene nanocomposite-coated stretchable fabric for wearable triboelectric nanogenerator and self-powered sensing applications. *Nano Energy.* **2022**;100: 107454.
53. Huang T, Zhang J, Yu B, Yu H, Long HR, Wang HZ, Zhang QH, Zhu MF. Fabric texture design for boosting the performance of a knitted washable textile triboelectric nanogenerator as wearable power. *Nano Energy.* **2019**;58:375.
54. Lin YY, Cheng NB, Meng N, Wang C, Wang XF, Yu JY, Ding B. A patterned knitted fabric with reversible gating stability for dynamic moisture management of human body. *Adv Funct Mater.* **2023**. <https://doi.org/10.1002/adfm.202304109>.
55. Li MQ, Xu BG, Li ZH, Gao YY, Yang YJ, Huang XX. Toward 3d double-electrode textile triboelectric nanogenerators for wearable biomechanical energy harvesting and sensing. *Chem Eng J.* **2022**;450: 137491.
56. Huang T, Wang C, Yu H, Wang HZ, Zhang QH, Zhu MF. Human walking-driven wearable all-fiber triboelectric nanogenerator containing electrospun polyvinylidene fluoride piezoelectric nanofibers. *Nano Energy.* **2015**;14:226.
57. Lee KY, Yoon H-J, Jiang T, Wen XN, Seung W, Kim S-W, Wang ZL. Fully packaged self-powered triboelectric pressure sensor using hemispheres-array. *Adv Energy Mater.* **2016**;6:1502566.
58. Liu LM, Pan J, Chen PN, Zhang J, Yu XH, Ding X, Wang BJ, Sun XM, Peng HS. A triboelectric textile templated by a three-dimensionally penetrated fabric. *J Mater Chem A.* **2016**;4:6077.
59. Zhou T, Zhang C, Han CB, Fan FR, Tang W, Wang ZL. Woven structured triboelectric nanogenerator for wearable devices. *ACS Appl Mater Interfaces.* **2014**;6:14695.
60. Tian ZM, He J, Chen X, Zhang ZX, Wen T, Zhai C, Han JQ, Mu JL, Hou XJ, Chou XJ, Xue CY. Performance-boosted triboelectric textile for harvesting human motion energy. *Nano Energy.* **2017**;39:562.
61. Rana SMS, Rahman MT, Zahed MA, Lee SH, Shin YD, Seonu S, Kim D, Salauddin M, Bhatta T, Sharshtha K, Park JY. Zirconium metal-organic framework and hybridized co-npc@mxene nanocomposite-coated fabric for stretchable, humidity-resistant triboelectric nanogenerators and self-powered tactile sensors. *Nano Energy.* **2022**;104: 107931.
62. Jiang CHZ, Lai CL, Xu BG, So MY, Li ZH. Fabric-rebound triboelectric nanogenerators with loops and layered structures for energy harvesting and intelligent wireless monitoring of human motions. *Nano Energy.* **2022**;93: 106807.
63. Cui NY, Liu JM, Gu L, Bai S, Chen XB, Qin Y. Wearable triboelectric generator for powering the portable electronic devices. *ACS Appl Mater Interfaces.* **2015**;7:18225.
64. Lv XS, Liu Y, Yu JY, Li ZL, Ding B. Smart fibers for self-powered electronic skins. *Adv Fiber Mater.* **2023**;5:401.
65. Wang ZL, Wang AC. On the origin of contact-electrification. *Mater Today.* **2019**;30:34.
66. Lin SQ, Xu L, Chi Wang A, Wang ZL. Quantifying electron-transfer in liquid-solid contact electrification and the formation of electric double-layer. *Nat Commun.* **2020**;11:399.
67. Apodaca MM, Wesson PJ, Bishop KJM, Ratner MA, Grzybowski BA. Contact electrification between identical materials. *Angew Chem Int Ed.* **2010**;49:946.
68. Baytekin HT, Patashinski AZ, Branicki M, Baytekin B, Soh S, Grzybowski BA. The mosaic of surface charge in contact electrification. *Science.* **2011**;333:308.
69. Sakaguchi M, Makino M, Ohura T, Iwata T. Contact electrification of polymers due to electron transfer among mechano anions, mechano cations and mechano radicals. *J Electrostat.* **2014**;72:412.
70. Zhan F, Wang AC, Xu L, Lin SQ, Shao JJ, Chen XY, Wang ZL. Electron transfer as a liquid droplet contacting a polymer surface. *ACS Nano.* **2020**;14:17565.
71. Pu X, Song WX, Liu MM, Sun CW, Du CH, Jiang CY, Huang X, Zou DC, Hu WG, Wang ZL. Wearable power-textiles by integrating fabric triboelectric nanogenerators and fiber-shaped dye-sensitized solar cells. *Adv Energy Mater.* **2016**;6:1601048.
72. Niu L, Wang J, Wang K, Pan H, Jiang GM, Chen CY, Ma PB. High-speed sirospun conductive yarn for stretchable embedded knitted circuit and self-powered wearable device. *Adv Fiber Mater.* **2023**;5:154.
73. Dong K, Deng JN, Ding WB, Wang AC, Wang PH, Cheng CY, Wang YC, Jin LM, Gu BH, Sun BZ, Wang ZL. Versatile core-sheath yarn for sustainable biomechanical energy harvesting and real-time human-interactive sensing. *Adv Energy Mater.* **2018**;8:1801114.
74. He M, Du WW, Feng YM, Li SJ, Wang W, Zhang X, Yu AF, Wan LY, Zhai JY. Flexible and stretchable triboelectric nanogenerator fabric for biomechanical energy harvesting and self-powered dual-mode human motion monitoring. *Nano Energy.* **2021**;86: 106058.
75. Kim KN, Chun JS, Kim JW, Lee KY, Park J-U, Kim S-W, Wang ZL, Baik JM. Highly stretchable 2d fabrics for wearable

- triboelectric nanogenerator under harsh environments. *ACS Nano.* **2015**;9:6394.
76. Zhou MJ, Xu F, Ma LY, Luo QL, Ma WW, Wang RW, Lan CT, Pu X, Qin XH. Continuously fabricated nano/micro aligned fiber based waterproof and breathable fabric triboelectric nanogenerators for self-powered sensing systems. *Nano Energy.* **2022**;104: 107885.
 77. Ye C, Xu QF, Ren J, Ling SJ. Violin string inspired core-sheath silk/steel yarns for wearable triboelectric nanogenerator applications. *Adv Fiber Mater.* **2020**;2:24.
 78. Zhao ZF, Pu X, Du CH, Li LX, Jiang CY, Hu WG, Wang ZL. Freestanding flag-type triboelectric nanogenerator for harvesting high-altitude wind energy from arbitrary directions. *ACS Nano.* **2016**;10:1780.
 79. Jing TT, Xu BG, Xin JH, Guan XY, Yang YJ. Series to parallel structure of electrode fiber: an effective method to remarkably reduce inner resistance of triboelectric nanogenerator textiles. *J Mater Chem A.* **2021**;9:12331.
 80. Zhu C, Wu JW, Yan JH, Liu XQ. Advanced fiber materials for wearable electronics. *Adv Fiber Mater.* **2023**;5:12.
 81. Pu X, Li LX, Liu MM, Jiang CY, Du CH, Zhao ZF, Hu WG, Wang ZL. Wearable self-charging power textile based on flexible yarn supercapacitors and fabric nanogenerators. *Adv Mater.* **2016**;28:98.
 82. Peng F, Liu D, Zhao W, Zheng GQ, Ji YX, Dai K, Mi LW, Zhang DB, Liu CT, Shen CY. Facile fabrication of triboelectric nanogenerator based on low-cost thermoplastic polymeric fabrics for large-area energy harvesting and self-powered sensing. *Nano Energy.* **2019**;65: 104068.
 83. Zhu MS, Huang Y, Ng WS, Liu JY, Wang ZF, Wang ZY, Hu H, Zhi CY. 3d spacer fabric based multifunctional triboelectric nanogenerator with great feasibility for mechanized large-scale production. *Nano Energy.* **2016**;27:439.
 84. Kim DK, Jeong JB, Lim K, Ko J, Lang P, Choi M, Lee S, Bae JH, Kim H. Improved output voltage of a nanogenerator with 3d fabric. *J Nanosci Nanotechnol.* **2020**;20:4666.
 85. Kang Y, Wang B, Dai SG, Liu GL, Pu YP, Hu CG. Folded elastic strip-based triboelectric nanogenerator for harvesting human motion energy for multiple applications. *ACS Appl Mater Interfaces.* **2015**;7:20469.
 86. Choi AY, Lee CJ, Park J, Kim D, Kim YT. Corrugated textile based triboelectric generator for wearable energy harvesting. *Sci Rep.* **2017**;7:45583.
 87. Lin ZM, Yang J, Li XS, Wu YF, Wei W, Liu J, Chen J, Yang J. Large-scale and washable smart textiles based on triboelectric nanogenerator arrays for self-powered sleeping monitoring. *Adv Funct Mater.* **2018**;28:1704112.
 88. Ning C, Dong K, Cheng RW, Yi J, Ye CY, Peng X, Sheng FF, Jiang Y, Wang ZL. Flexible and stretchable fiber-shaped triboelectric nanogenerators for biomechanical monitoring and human-interactive sensing. *Adv Funct Mater.* **2021**;31:2006679.
 89. Zhang DW, Yang WF, Gong W, Ma WW, Hou CY, Li YG, Zhang QH, Wang HZ. Abrasion resistant/waterproof stretchable triboelectric yarns based on fermat spirals. *Adv Mater.* **2021**;33:2100782.
 90. Kavarthupu VS, Graham SA, Manchi P, Paranjape MV, Yu JS. Electrospun znsno3/pvdf-hfp nanofibrous triboelectric films for efficient mechanical energy harvesting. *Adv Fiber Mater.* **2023**. <https://doi.org/10.1007/s42765-023-00295-3>.
 91. Fan JC, Yuan MM, Wang LB, Xia QX, Zheng HW, Zhou AG. Mxene supported by cotton fabric as electrode layer of triboelectric nanogenerators for flexible sensors. *Nano Energy.* **2023**;105: 107973.
 92. Kwak SS, Kim H, Seung W, Kim J, Hinche R, Kim S-W. Fully stretchable textile triboelectric nanogenerator with knitted fabric structures. *ACS Nano.* **2017**;11:10733.
 93. Liu LQ, Yang XY, Zhao LL, Xu WK, Wang JW, Yang QM, Tang QW. Nanowrinkle-patterned flexible woven triboelectric nanogenerator toward self-powered wearable electronics. *Nano Energy.* **2020**;73: 104797.
 94. Feng LL, Xu SJ, Sun T, Zhang CJ, Feng JD, Yao LR, Ge JL. Fire/acid/alkali-resistant aramid/carbon nanofiber triboelectric nanogenerator for self-powered biomotion and risk perception in fire and chemical environments. *Adv Fiber Mater.* **2023**. <https://doi.org/10.1007/s42765-023-00288-2>.
 95. Niu L, Peng X, Chen LJ, Liu Q, Wang TR, Dong K, Pan H, Cong HL, Liu GL, Jiang GM, Chen CY, Ma PB. Industrial production of bionic scales knitting fabric-based triboelectric nanogenerator for outdoor rescue and human protection. *Nano Energy.* **2022**;97: 107168.
 96. Dong K, Wang YC, Deng JN, Dai YJ, Zhang SL, Zou HY, Gu BH, Sun BZ, Wang ZL. A highly stretchable and washable all-yarn-based self-charging knitting power textile composed of fiber triboelectric nanogenerators and supercapacitors. *ACS Nano.* **2017**;11:9490.
 97. Mather RR, Wilson JIB. Fabrication of photovoltaic textiles. *Coatings.* **2017**. <https://doi.org/10.3390/coatings7050063>.
 98. Zhang HL, Yang Y, Hou T-C, Su YJ, Hu CG, Wang ZL. Triboelectric nanogenerator built inside clothes for self-powered glucose biosensors. *Nano Energy.* **2013**;2:1019.
 99. Hou T-C, Yang Y, Zhang HL, Chen J, Chen L-J, Lin WZ. Triboelectric nanogenerator built inside shoe insole for harvesting walking energy. *Nano Energy.* **2013**;2:856.
 100. Jung S, Lee J, Hyeon T, Lee M, Kim D-H. Fabric-based integrated energy devices for wearable activity monitors. *Adv Mater.* **2014**;26:6329.
 101. He J, Qian S, Niu XS, Zhang N, Qian JC, Hou XJ, Mu JL, Geng WP, Chou XJ. Piezoelectric-enhanced triboelectric nanogenerator fabric for biomechanical energy harvesting. *Nano Energy.* **2019**;64: 103933.
 102. Guo YB, Li KR, Hou CY, Li YG, Zhang QH, Wang HZ. Fluoro-alkylsilane-modified textile-based personal energy management device for multifunctional wearable applications. *ACS Appl Mater Interfaces.* **2016**;8:4676.
 103. Wang SH, Lin L, Wang ZL. Nanoscale triboelectric-effect-enabled energy conversion for sustainably powering portable electronics. *Nano Lett.* **2012**;12:6339.
 104. Yang YQ, Sun N, Wen Z, Cheng P, Zheng HC, Shao HY, Xia YJ, Chen C, Lan HW, Xie XK, Zhou CJ, Zhong J, Sun XH, Lee S-T. Liquid-metal-based super-stretchable and structure-designable triboelectric nanogenerator for wearable electronics. *ACS Nano.* **2027**;2018:12.
 105. Lee J, Kwon H, Seo J, Shin S, Koo JH, Pang CH, Son S, Kim JH, Jang YH, Kim DE, Lee T. Conductive fiber-based ultrasensitive textile pressure sensor for wearable electronics. *Adv Mater.* **2015**;27:2433.
 106. Ming XQ, Shi L, Zhu H, Zhang Q. Stretchable, phase-transformable ionogels with reversible ionic conductor-insulator transition. *Adv Funct Mater.* **2020**;30:2005079.
 107. Park H, Oh S-J, Kim D, Kim M, Lee C, Joo H, Woo I, Bae JW, Lee J-H. Plasticized pvc-gel single layer-based stretchable triboelectric nanogenerator for harvesting mechanical energy and tactile sensing. *Adv Sci.* **2022**;9:2201070.
 108. Sun LJ, Huang HF, Ding QY, Guo YF, Sun W, Wu ZC, Qin ML, Guan QB, You ZW. Highly transparent, stretchable, and self-healable ionogel for multifunctional sensors, triboelectric nanogenerator, and wearable fibrous electronics. *Adv Fiber Mater.* **2022**;4:98.
 109. Chu H, Jang H, Lee Y, Chae Y, Ahn J-H. Conformal, graphene-based triboelectric nanogenerator for self-powered wearable electronics. *Nano Energy.* **2016**;27:298.

110. Dong L, Wang MX, Wu JJ, Zhu CH, Shi J, Morikawa H. Deformable textile-structured triboelectric nanogenerator knitted with multifunctional sensing fibers for biomechanical energy harvesting. *Adv Fiber Mater.* **2022**;4:1486.
111. Jing TT, Wang SC, Yuan HY, Yang YJ, Xue M, Xu BG. Interfacial roughness enhanced gel/elastomer interfacial bonding enables robust and stretchable triboelectric nanogenerator for reliable energy harvesting. *Small.* **2023**;19:2206528.
112. Liu YH, Fu Q, Mo JL, Lu YX, Cai CC, Luo B, Nie SX. Chemically tailored molecular surface modification of cellulose nanofibrils for manipulating the charge density of triboelectric nanogenerators. *Nano Energy.* **2021**;89: 106369.
113. Mishra S, Supraja P, Haranath D, Kumar RR, Pola S. Effect of surface and contact points modification on the output performance of triboelectric nanogenerator. *Nano Energy.* **2022**;104: 107964.
114. Zhu ML, Shi QF, He TY, Yi ZR, Ma YM, Yang B, Chen T, Lee CK. Self-powered and self-functional cotton sock using piezoelectric and triboelectric hybrid mechanism for healthcare and sports monitoring. *ACS Nano.* **1940**;2019:13.
115. Salauddin M, Rana SMS, Sharifuzzaman M, Rahman MT, Park C, Cho H, Maharjan P, Bhatta T, Park JY. A novel mxene/eco-flex nanocomposite-coated fabric as a highly negative and stable friction layer for high-output triboelectric nanogenerators. *Adv Energy Mater.* **2021**;11:2002832.
116. Xiong JQ, Cui P, Chen XL, Wang JX, Parida K, Lin MF, Lee PS. Skin-touch-actuated textile-based triboelectric nanogenerator with black phosphorus for durable biomechanical energy harvesting. *Nat Commun.* **2018**;9:4280.
117. Wu RH, Liu S, Lin ZF, Zhu SH, Ma LY, Wang ZL. Industrial fabrication of 3d braided stretchable hierarchical interlocked fancy-yarn triboelectric nanogenerator for self-powered smart fitness system. *Adv Energy Mater.* **2022**;12:2201288.
118. Ning C, Cheng RW, Jiang Y, Sheng FF, Yi J, Shen S, Zhang YH, Peng X, Dong K, Wang ZL. Helical fiber strain sensors based on triboelectric nanogenerators for self-powered human respiratory monitoring. *ACS Nano.* **2022**;16:2811.
119. Zou Y, Tan PC, Shi BJ, Ouyang H, Jiang DJ, Liu Z, Li H, Yu M, Wang C, Qu XC, Zhao LM, Fan YB, Wang ZL, Li Z. A bionic stretchable nanogenerator for underwater sensing and energy harvesting. *Nat Commun.* **2019**;10:2695.
120. Ma LY, Wu RH, Patil A, Yi J, Liu D, Fan XW, Sheng FF, Zhang YF, Liu S, Shen S, Wang J, Wang ZL. Acid and alkali-resistant textile triboelectric nanogenerator as a smart protective suit for liquid energy harvesting and self-powered monitoring in high-risk environments. *Adv Funct Mater.* **2021**;31:2102963.
121. Cheng RW, Dong K, Liu LX, Ning C, Chen PF, Peng X, Liu D, Wang ZL. Flame-retardant textile-based triboelectric nanogenerators for fire protection applications. *ACS Nano.* **2020**;14:15853.
122. Lai Y-C, Hsiao Y-C, Wu H-M, Wang ZL. Waterproof fabric-based multifunctional triboelectric nanogenerator for universally harvesting energy from raindrops, wind, and human motions and as self-powered sensors. *Adv Sci.* **2019**;6:1801883.
123. Wang ZZ, Gong LK, Dong SC, Fan BB, Feng Y, Zhang Z, Zhang C. A humidity-enhanced silicon-based semiconductor tribovoltaic direct-current nanogenerator. *J Mater Chem A.* **2022**;10:25230.
124. Liu D, Zhou LL, Cui SN, Gao YK, Li SX, Zhao ZH, Yi ZY, Zou HY, Fan YJ, Wang J, Wang ZL. Standardized measurement of dielectric materials' intrinsic triboelectric charge density through the suppression of air breakdown. *Nat Commun.* **2022**;13:6019.
125. Chen CY, Guo HY, Chen LJ, Wang YC, Pu XJ, Yu WD, Wang FM, Du ZQ, Wang ZL. Direct current fabric triboelectric nanogenerator for biomotion energy harvesting. *ACS Nano.* **2020**;14:4585.
126. Shao H, Fang J, Wang HX, Niu HT, Zhou H, Cao YY, Chen FY, Fu SD, Lin T. Schottky direct-current energy harvesters with large current output density. *Nano Energy.* **2019**;62:171.
127. Liu GX, Luan RF, Qi YC, Gong LK, Cao J, Wang ZH, Liu F, Zeng JH, Huang XL, Qin YH, Dong SC, Feng Y, Huang LB, Zhang C. Organic tribovoltaic nanogenerator with electrically and mechanically tuned flexible semiconductor textile. *Nano Energy.* **2023**;106: 108075.
128. Wei CH, Cheng R, Ning C, Wei X, Peng X, Lv TM, Sheng FF, Dong K, Wang ZL. A self-powered body motion sensing network integrated with multiple triboelectric fabrics for biometric gait recognition and auxiliary rehabilitation training. *Adv Funct Mater.* **2023**. <https://doi.org/10.1002/adfm.202303562>.
129. He HL, Liu JR, Wang YS, Zhao YH, Qin Y, Zhu ZY, Yu ZC, Wang JF. An ultralight self-powered fire alarm e-textile based on conductive aerogel fiber with repeatable temperature monitoring performance used in firefighting clothing. *ACS Nano.* **2022**;16:2953.
130. Ye GM, Wan YF, Wu JM, Zhuang WB, Zhou ZQ, Jin TS, Zi JY, Zhang DD, Geng XM, Yang P. Multifunctional device integrating dual-temperature regulator for outdoor personal thermal comfort and triboelectric nanogenerator for self-powered human-machine interaction. *Nano Energy.* **2022**;97: 107148.
131. Yi J, Dong K, Shen S, Jiang Y, Peng X, Ye CY, Wang ZL. Fully fabric-based triboelectric nanogenerators as self-powered human-machine interactive keyboards. *Nano Micro Lett.* **2021**;13:103.

Publisher's Note Springer Nature remains neutral with regard to jurisdictional claims in published maps and institutional affiliations.

Springer Nature or its licensor (e.g. a society or other partner) holds exclusive rights to this article under a publishing agreement with the author(s) or other rightsholder(s); author self-archiving of the accepted manuscript version of this article is solely governed by the terms of such publishing agreement and applicable law.



Dali Yan is a postgraduate in the School of Materials Science and Engineering at Wuhan Textile University under the supervision of Prof. Bo Deng. He received his B.S. degree from the School of Electrical and Information Engineering, Dezhou University, in 2021. His current scientific interests are focused on textile-based triboelectric nanogenerator.



Jian Ye was drafted into the military in 2017, graduated from Wuhan University of Science and Technology City College with a bachelor's degree in 2022. Currently, he is a full-time graduate student in the School of Materials and Engineering, Wuhan Textile University. His current scientific interests are focused on woven-structure-based triboelectric nanogenerator.



Yahui Zhou is a postgraduate at Wuhan Textile University, Institute of Technology, supervised by Prof. Bo Deng. He received his B.S. degree in Environmental Engineering from Guangxi University for Nationalities in 2021, and his current scientific interests are focused on visible light catalyst loading on fabrics.



Xingxin Lei was born in Guizhou, China, and graduated from Changzhou University with a B.E. He has studied under Prof. Deng Bo at Wuhan Textile University since 2022. His main research interests are functional fibers and textiles.



Bo Deng is a professor at the School of Materials Science and Engineering, Wuhan Textile University. He received his Ph.D. degree from Shanghai Institute of Applied Physics, Chinese Academy of Sciences (CAS) in 2008. From 2008 to 2011, he worked as an associate researcher at the Shanghai Institute of Applied Physics, Chinese Academy of Sciences (CAS). From 2011 to 2012, he was a guest scientist with the Paul Scherrer Institute, Switzerland. From 2012 to 2015, he worked

as a post-doctoral researcher at the University of British Columbia, Canada. He is mainly engaged in the fundamental and application research of inorganic nanomaterials-modified functional fabrics.



Weilin Xu received the Ph.D. degree in textile material from Donghua University, Shanghai, China, in 1997. From 1997 to 1999, he joined the State Key Laboratory of Polymer Materials Engineering, Sichuan University, Sichuan, China, as a post-doctoral. From 1999 to 2000, he was a visiting researcher with the Hong Kong Polytechnic University, China. His research interests are intelligent spinning, advanced processing technology, etc. He is currently the director of the State Key Laboratory of

New Textile Materials and Advanced Processing Technologies since 2021. He was elected as a Member of the Chinese Academy of Engineering, in 2021.